University of Alberta
Printing Department

THE UNIVERSITY OF ALBERTA

A STUDY OF HEAT CONDUCTION WITH PHASE CHANGE

by

JAMES R. GUNDERSON, B.Sc. (Alberta)

A THESIS

SUBMITTED TO THE FACULTY OF GRADUATE STUDIES

IN PARTIAL FULFILMENT OF THE REQUIREMENTS FOR THE DEGREE

OF MASTER OF SCIENCE

DEPARTMENT OF MECHANICAL ENGINEERING

EDMONTON, ALBERTA

July 1966

UNIVERSITY OF ALBERTA

FACULTY OF GRADUATE STUDIES

The undersigned certify that they have read, and recommend to the Faculty of Graduate Studies for acceptance, a thesis entitled "A STUDY OF HEAT CONDUCTION WITH PHASE CHANGE" submitted by JAMES R. GUNDERSON in partial fulfilment of the requirements for the degree of Master of Science.

ABSTRACT

The dimensionless form of the conduction equation presented in this thesis is mathematically linear and has been applied, in the past, to several fixed boundary conditions. With phase change, the overall problem is non-linear in nature. The reason for this is that one boundary is moving continuously and its position is not known a priori.

A theoretical and experimental investigation is presented for freezing or melting in one dimension when the boundary temperature varies with time. An explicit solution and an alternative quadrature solution is given for the semi-infinite domain when the boundary temperature varies as a simple power of time. Experimental results, for an ice-water system, are presented for particular values of this power and are compared with predictions from the quadrature solution. The simple power law solution has been extended, in approximate form, to predict depth of freezing and melting during one cycle of a sinusoidal surface temperature. Comparison with experimental results shows qualitative agreement and furnishes new insight into the problem of periodic freezing and melting.

Experiments in two-dimensional ice formation are included. Typical ice profiles are presented for the case of two surfaces at different uniform temperatures with one surface held below the freezing temperature.

ACKNOWLEDGEMENTS

The author wishes to thank the following for their contributions:

- Dr. G.S.H. Lock for suggesting an interesting research topic and supervising the thesis,
- Mr. H. Golls who built the experimental apparatus and members of the Mechanical Engineering Shop who aided in the construction,
- Miss Lynne Fiveland for typing the thesis,
- the National Research Council for the funds made available under Grant No. A-1672,
- my wife, Marguerite, for her understanding and patience during the last two years.

TABLE OF CONTENTS

LIST OF FIGURES

LIST OF TABLES

NOMENCLATURE

θ, ψ, f	temperature
Φ	reciprocal temperature constant as defined
τ, t	time
x	distance from domain edge
β, b	interface depth
η	similarity variable
ξ	dummy variable
n	temperature index (power exponent of time)
S	Laplace transformation variable
P, Q,	functions of η defined in text
a, A, B, C	constants
K	thermal conductivity
c_p	specific heat
L	latent heat of fusion
ρ	density
κ	thermal diffusivity
Γ	gamma function
ω	angular velocity
α	radians
', ''	first and second derivatives (with respect to η)
-	Laplace transform with respect to time.

SUBSCRIPTS

o	location x = o
i	initial condition
m, c	maximum

CHAPTER I

INTRODUCTION

When a liquid undergoes an unsteady change to the solid phase, thermal energy in the form of latent heat of fusion is released at the moving liquid-solid interface, the history of which is unknown a priori. This latter peculiarity gives the problem a mathematically non-linear character and relatively simple analytic solutions are difficult to obtain.

More than a century ago, Neumann (Carslaw and Jaeger [1]*) found an exact solution relating to the solidification of the semi-infinite region of liquid initially above or at the stable crystallization (freezing) temperature with the boundary temperature suddenly decreased to and maintained at a temperature below freezing. Stefan [2] (Ingersoll [3]) later published the solution for the simpler situation when the region is initially at the freezing temperature. The literature frequently refers to the subject as the Stefan problem.

With increasing interest in the casting of metals, Lightfoot [4] found an approximate solution for the case of the slab of finite thickness, using the Neumann boundary

---

* Numbers in brackets denote references given on page 69.

conditions; it was shown that the velocity of the interface was practically constant upon approaching the centre of the slab. As a comparison, this thesis contains the results of an experiment using a slab insulated on one surface and with a time dependent temperature condition on the other. A more recent extension was given by Kreith and Romie [5] who considered a constant fusion velocity for cylinders and spheres; in addition they considered the semi-infinite domain and the equation for interface depth, β, in a dimensionless form which is identical to the equation termed the Neumann solution in this thesis.

In 1950, Landau [6] formulated the governing equations in general form and used a finite difference procedure to present a set of solutions for the semi-infinite region; this work has, in the past, been used as a standard for comparison purposes. In 1959, Murray and Landis [7] extended the range of initial and boundary conditions with a numerical approach permitting a continuous determination of the fusion front travel and indicating the internal temperature distribution with good accuracy.

Several diversified approaches have been presented in solving for specific boundary and initial conditions. Goodman [8] introduced the heat balance integral following the momentum integral principle of von Karman. The concept

makes use of a second order polynomial to describe an assumed temperature distribution in the solid region; if the assumption is correct, accurate analytical solutions will result. Poots [9,10] used integral methods to satisfy the boundary conditions for one- and two-dimensional phase change problems. The method may be useful for theoretical comparison with the two-dimensional experiments given in this thesis.

The mathematical generalization of the Neumann-Stefan problem, assuming the boundary temperature as an arbitrary function of time, was originated by Portnov [11] in 1962. The initial temperature distribution, an arbitrary function of distance, is included in the Laplace-integral solution. The method attacks the problem directly but Westphal [12] shows that its application to Arctic ice formation is extremely difficult. The resulting power series appears to be suitable for numerical computer programming for various boundary conditions.

The purpose of this thesis is to present an "intermediate" analytical solution extending the basic work of Neumann and yet not having the complexity of the Portnov generalization. The solution mathematically describes the solid region temperature and interface location in dimensionless form employing a simple, time-dependent boundary condition. Only the case of the liquid

initially at the freezing temperature is considered. The solution is

(1) in explicit form convenient for application with standard tables and,

(2) in quadrature form for computer calculation of intermediate points not obtainable by the explicit solution.

A numerical comparison of the explicit and quadrature solution is included as Appendix B. An application of the Laplace-integral method is presented as Appendix C for comparison with the explicit solution using a linear temporal variation in boundary temperature. In addition, the case of the sinusoidual boundary temperature has been considered; an approximate solution is obtained for temperature and interface depth using superposition of explicit solutions.

An explicit solution is also obtainable for the case of the liquid region initially at a uniform temperature above freezing but is not presented in this thesis. The case of an initially non-uniform temperature in the liquid has not been investigated.

Experimental results show good agreement with theory using an ice-water system and simple time-dependent boundary conditions. Qualitative agreement is shown for the sinusoidual boundary condition. As a natural extension of the unidimensional problem, experimental results for

the two-dimensional steady state case have been included. For completeness, a brief experimental analysis of supercooling is presented.

CHAPTER II

ONE-DIMENSIONAL THEORY

2.1 FORMULATION OF THE PHASE CHANGE PROBLEM

Consider the semi-infinite domain ($x > 0$) shown in figure 2.1. Let the initial temperature of the liquid domain, in this case water, be at the melting temperature which shall be considered the temperature datum. The melting temperature is used as the fixed reference since the "freezing" temperature is variable with the effect of supercooling. When the surface temperature $\theta_o(t)$ is lowered then, ideally, ice will form as shown. If the ice properties are assumed to be constant, the differential equation governing heat conduction within the ice region is given by

$$\frac{\partial^2\theta}{\partial x^2} - \frac{1}{\kappa}\frac{\partial\theta}{\partial t} = 0 \qquad (1)$$

Mathematically, then, the problem consists of determining the solution to equation (1) subject to the initial condition $\theta_i(x) = 0$ and boundary conditions

$$\begin{aligned} x &= 0 \quad ; \quad \theta = \theta_o(t) \\ x &= b(t); \quad \theta = 0 \end{aligned} \qquad (2)$$

where $b(t)$ is the ice depth. Although the time dependent boundary condition at the origin may take many different

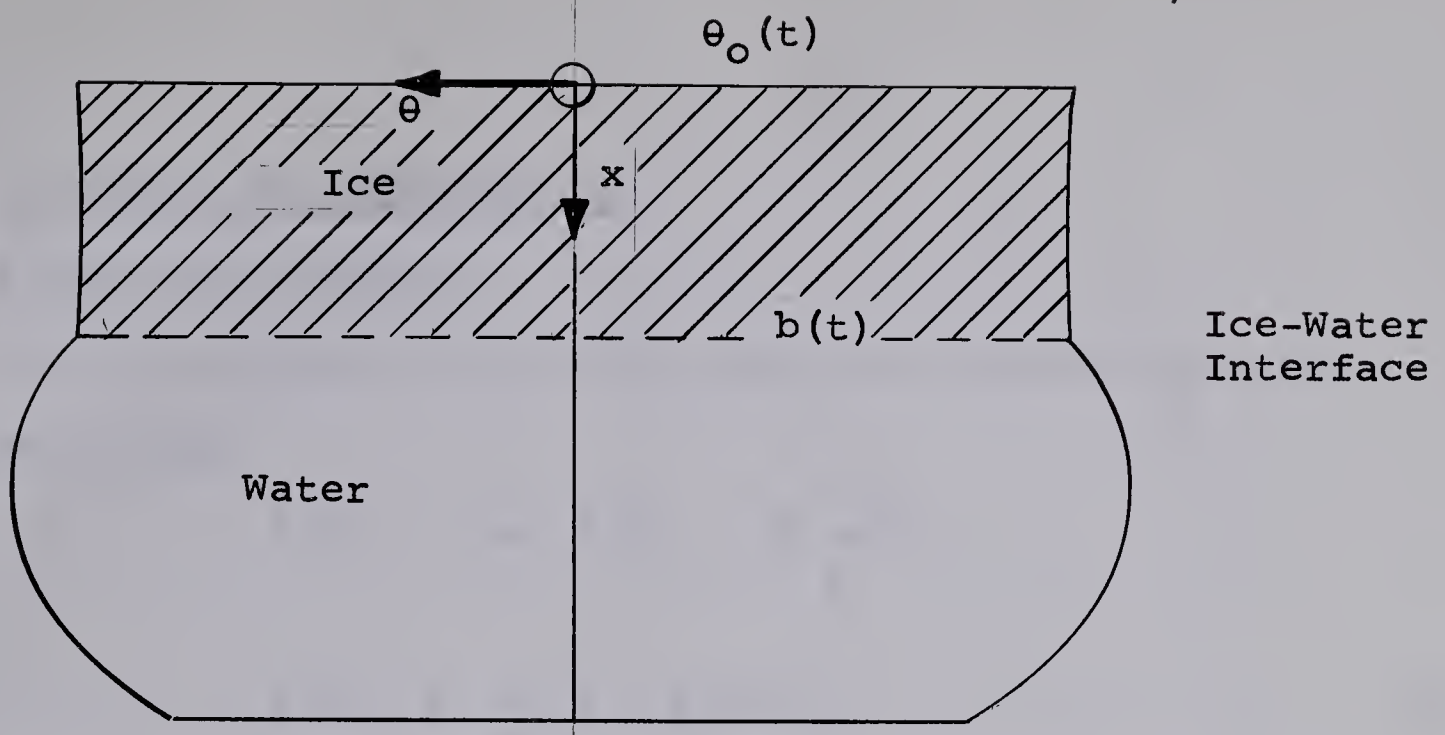

FIG. 2.1 ONE-DIMENSIONAL DOMAIN

forms in practice, the surface temperature will be restricted to the form $\theta_o(t) = Ct^n$ where C and n are constants. Using this surface temperature variation, a closed solution for ice depth is developed.

Taking the similarity forms for the ice region as

$$\theta(\eta) = Ct^n f_n(\eta) \tag{3}$$

where $\eta = x/2\sqrt{\kappa t}$,

then, equation (1) may be transformed into the linear ordinary differential equation

$$f'' + 2\eta f' - 4nf = 0 \tag{4}$$

with transformed boundary conditions

$$f(0) = 1,\ f(\beta) = 0 \tag{5}$$

where $\beta = b(t)/2\sqrt{\kappa t}$,

which is the dimensionless ice depth.

2.2 SOLUTION FOR TEMPERATURE

2.2-1 Explicit Solution

If ψ is a solution of (4), then the complete solution may be written

$$f(\eta) = A\psi + B\psi \int \frac{e^{-\eta^2} d\eta}{\psi^2}$$

or

$$f(\eta) = \psi \left[A + BP(\eta) \right] \tag{6}$$

A known solution for ψ, using the surface temperature $\theta_o(t) = Ct^n$, is

$$\psi(\eta) = 2^{2n}\, \Gamma(n+1)\, i^{2n}\mathrm{erfc}\eta \,. \tag{7}$$

Substituting the known solution (7) into equation (6), and satisfying the boundary conditions (5), yields the temperature in the frozen region as

$$f_n(\eta) = 2^{2n}\, \Gamma(n+1)\, i^{2n}\mathrm{erfc}\eta \left[1 - \frac{Pn(\eta)}{P_n(\beta)} \right] \tag{8}$$

where

$$P_n(\eta) = \int_o^\eta \frac{e^{-\xi^2} d\xi}{(i^{2n}\mathrm{erfc}\ \xi)^2} \tag{9}$$

For the Neumann problem, the integer value n = 0 is substituted into equation (9) giving

$$P_o(\eta) = \frac{\sqrt{\pi}}{2} \frac{\mathrm{erf}\eta}{\mathrm{erfc}\eta} \tag{10}$$

Using (10) in equation (8), the Neumann solution for temperature is

$$f_o(\eta) = 1 - \frac{\mathrm{erf}\eta}{\mathrm{erf}\beta} \tag{11}$$

Evaluation of the integral (9) for a number of integer values $2n = 1,2,\ldots$ has been undertaken by the author and is presented in table 2.1. To evaluate $Pn(\eta)$, the recurrence formula

$$i^n\text{erfc}\ \xi = \frac{1}{2n}\left(i^{n-2}\text{erfc}\ \xi - 2\xi i^{n-1}\text{erfc}\ \xi\right)$$

is expanded term by term and then groupings made of the coefficients of $e^{-\xi^2}$ and erfc ξ in the numerator of the equation

$$dP_n(\xi) = \frac{e^{-\xi^2}d\xi}{(i^{2n}\text{erfc}\ \xi)^2}$$

where $P_n(\xi) = \frac{u}{v}$ and $v = i^{2n}\text{erfc}\ \xi$.

Hence, the numerator is considered to take the form,

$$e^{-\xi^2} = \left(i^{2n}\text{erfc}\ \xi\right)\frac{du}{d\xi} + \left(i^{2n-1}\text{erfc}\ \xi\right)u\ ,$$

where the necessary value of u must be determined.

2n	Pn(η)
0	$P_o(\eta) = \frac{\sqrt{\pi}}{2} \frac{\text{erf}\eta}{\text{erfc}\eta}$
1	$P_{1/2}(\eta) = \frac{\sqrt{\pi}\ \eta}{\text{ierfc}\eta}$
2	$P_1(\eta) = \frac{\sqrt{\pi}\ (2\eta^2 + 1)}{i^2\text{erfc}\eta} - 4\sqrt{\pi}$
3	$P_{3/2}(\eta) = \frac{2\sqrt{\pi}\ (2\eta^3 + 3\eta)}{i^3\text{erfc}\eta}$
4	$P_2(\eta) = \frac{2\sqrt{\pi}\ (4\eta^4 + 12\eta^2 + 3)}{i^4\text{erfc}\eta} - 192\sqrt{\pi}$
5	$P_{5/2}(\eta) = \frac{4\sqrt{\pi}\ (4\eta^5 + 20\eta^3 + 15\eta)}{i^5\text{erfc}\eta}$
6	$P_3(\eta) = \frac{4\sqrt{\pi}\ (8\eta^6 + 60\eta^4 + 90\eta^2 + 15)}{i^6\text{erfc}\eta} - \frac{60\sqrt{\pi}}{i^6\text{erfc}\ 0}$

TABLE 2.1 TABULATION OF $P_n(\eta)$

2.2-2 Quadrature Solution

If 2n is not a positive integer, computation of the temperature may be executed in quadrature form. Considering equation (4) and using an integrating factor, it may be written

$$\frac{d}{d\eta} \left[f'(\eta)\, e^{\int 2\eta d\eta} \right] = 4nf(\eta)\, e^{\int 2\eta d\eta} \tag{12}$$

Integrating (12) twice and imposing the boundary conditions (5) yields the solution

$$f_n(\eta) = 1 - \frac{\text{erf}\eta}{\text{erf}\beta} + 4n \left[Q(\eta) - \frac{\text{erf}\eta}{\text{erf}\beta}\, Q(\beta) \right] \tag{13}$$

where $$Q(\eta) = \int_0^{\eta} e^{-\xi^2} \int_0^{\xi} f_n(\xi)\, e^{\xi^2}\, d\xi\, d\xi . \tag{14}$$

The Neumann solution is recovered by putting n = 0.

Equations (8) and (13) represent the formal solution for the temperature distribution in the ice region with the selected surface temperature variation, $\theta_o(t) = Ct^n$.

A computer programme in Fortran IV language was written to evaluate the temperature function (13). The computation was carried out on an IBM 7040-1401 machine in the Department of Computing Science, University of Alberta. Appendix A provides the programme. The computer data results are plotted in figures 2.2, 2.3, and 2.4.

In discussing the temperature function (13), it should be noted that $Q(\eta)$ is bounded in the range

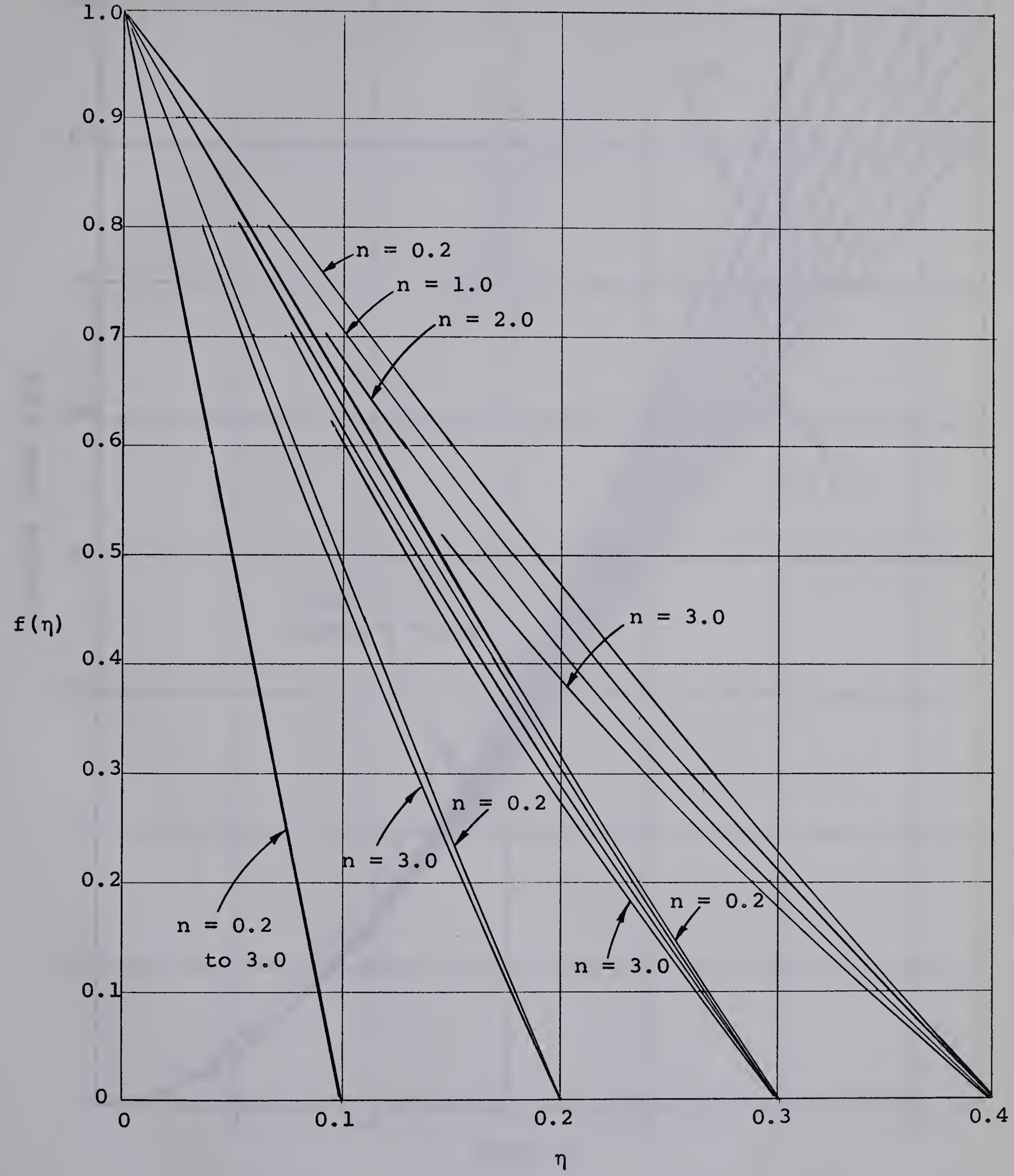

FIG. 2.2 THEORETICAL TEMPERATURE PROFILES

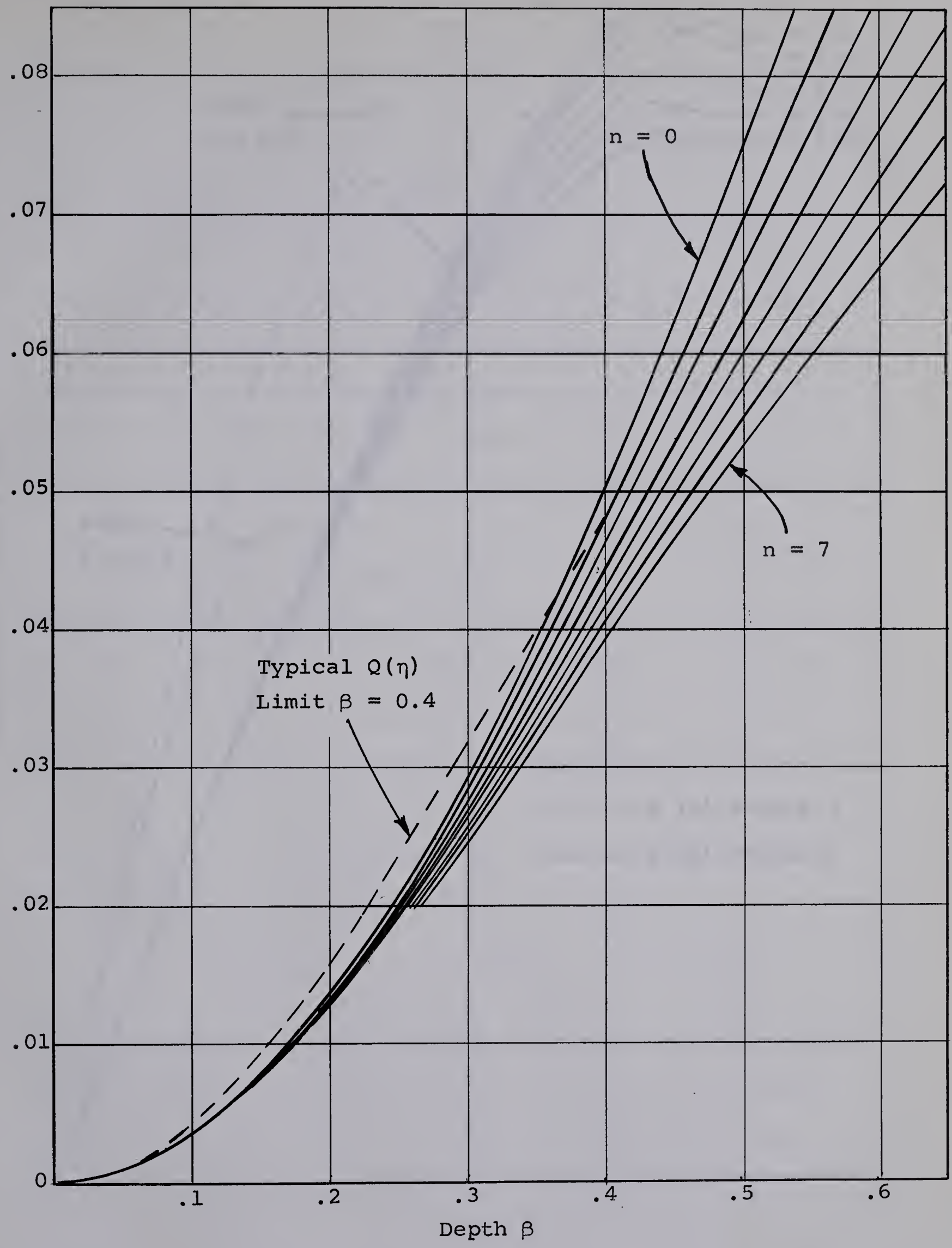

FIG. 2.3 INTEGRAL Q(β) VERSUS DEPTH β

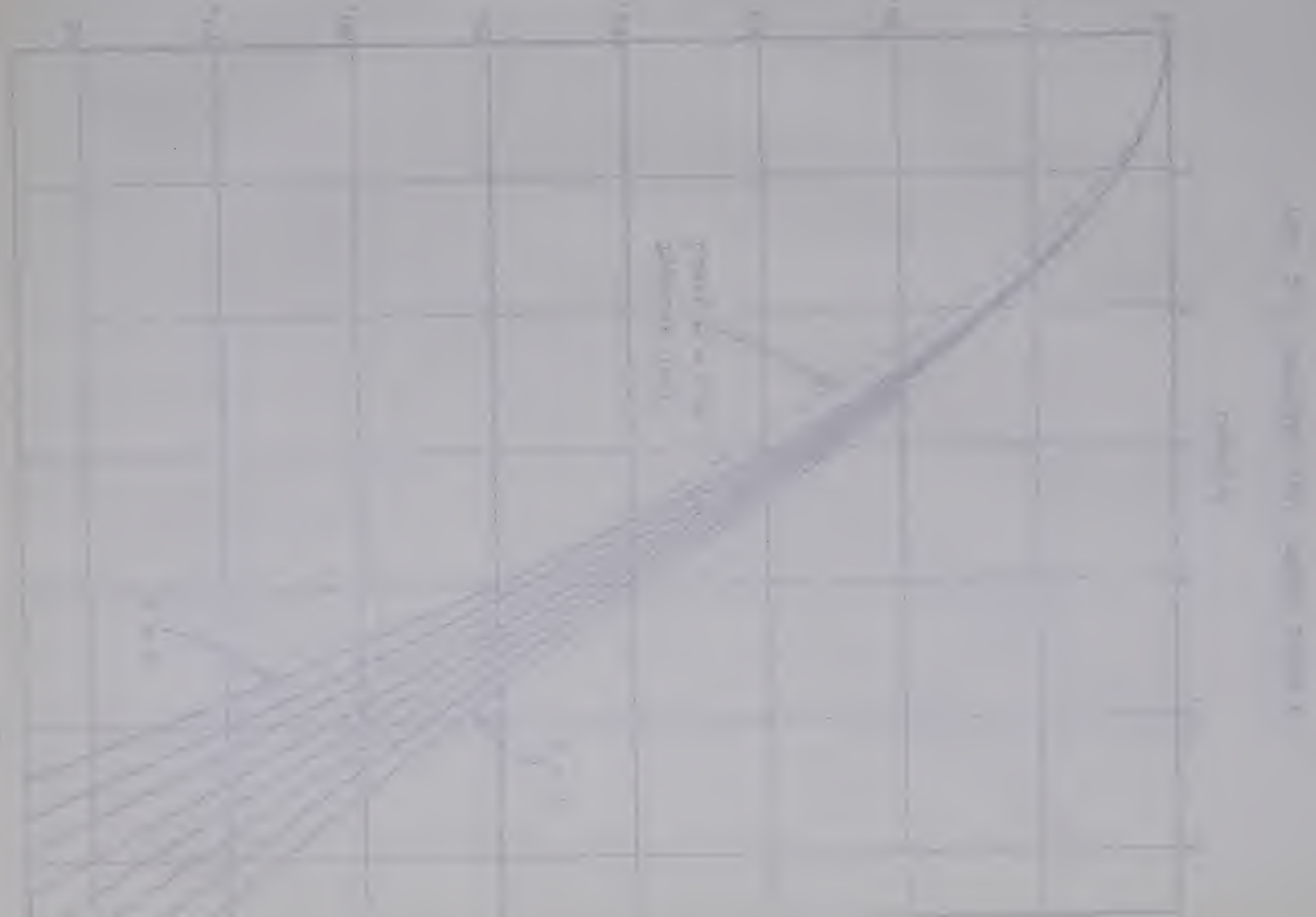

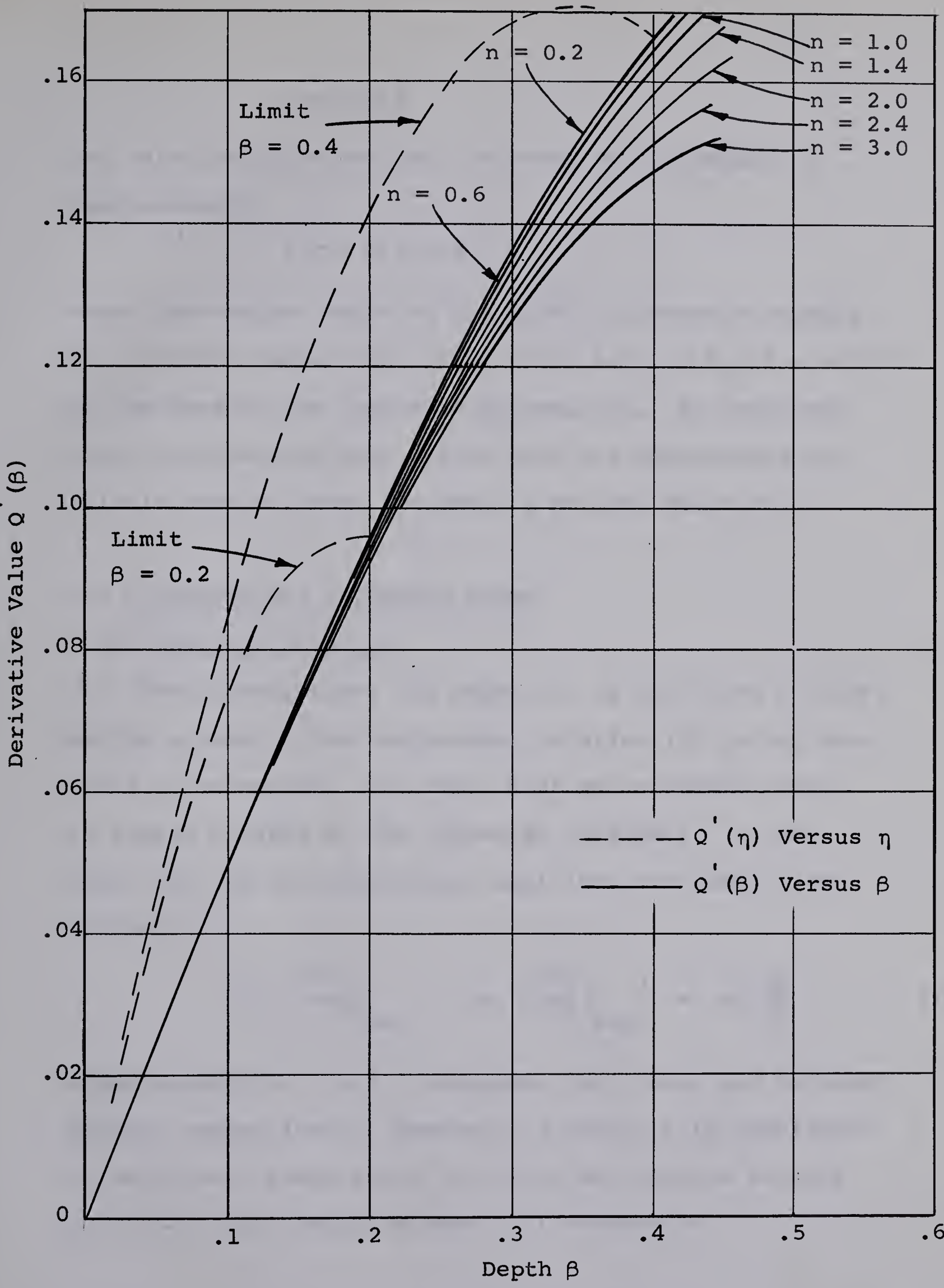

FIG. 2.4 DERIVATIVE Q' (β) VERSUS DEPTH β

$$o < \eta < \beta$$

and calculations show that the range of the domain is approximately

$$o < \beta < 0.765$$

where the maximum value of $\beta = 0.765$ corresponds roughly to a surface temperature of absolute zero or $\theta_o(t) = -492\,^{\circ}F$ in the case of ice (refer to Appendix D). An important point to note from Fig. 2.2 is that the temperature profile is nearly linear for small β and any value of n.

2.3 SOLUTION FOR INTERFACE DEPTH

2.3-1 Explicit Solution

The dimensionless ice depth, β, is not known a priori and as a result, the temperature solution (8) is not complete as presented. Ice depth must be determined from an energy balance at the ice-water interface. In general, for the uni-dimensional semi-infinite domain, the balance is

$$-\left[K_1 \left(\frac{\partial \theta_1}{\partial x}\right)_{x=b} - K_2 \left(\frac{\partial \theta_2}{\partial x}\right)_{x=b}\right] = \rho L \frac{db}{dt} \qquad (15)$$

where subscripts 1 and 2 represent the frozen and unfrozen regions respectively. However, if region 2 is considered to be at zero temperature initially and remains at zero for $t > o$, the energy balance (15) reduces to

$$-K\left(\frac{\partial\theta}{\partial x}\right)_{x=b} = \rho L \frac{db}{dt} \tag{16}$$

where the subscripts are deleted for convenience. The temperature gradient at the edge of the ice domain is

$$\left(\frac{\partial\theta}{\partial x}\right)_{x=b} = \frac{\theta_o f_n'(\beta)}{2\sqrt{\kappa\ t}} \tag{17}$$

The dimensionless temperature gradient at β may be obtained by differentiating (8) which yields

$$f_n'(\beta) = \frac{-2^{2n}\Gamma(n+1)\ i^{2n}\text{erfc}\ \beta\ P'n(\beta)}{P_n(\beta)} \tag{18}$$

where $P_n'(\beta)$ is found directly from equation (9). Substitution of equation (18) into (17) and hence (16) gives the ice front velocity as

$$\frac{db}{dt} = \frac{K}{\rho L}\ \frac{\theta_o}{2\sqrt{\kappa t}}\ \ \frac{2^{2n}\ \Gamma(n+1)\ e^{-\beta^2}}{P_n(\beta)\ i^{2n}\text{erfc}\ \beta} \tag{19}$$

where $P_n(\beta)$ may be obtained from table 2.1.

If equation (19) is written in the original form

$$\frac{db}{dt} = 2a\sqrt{\kappa}\ \ t^{n-1/2}\ f_n'(\beta)\ , \tag{20}$$

where $a = -CpC/4L$, then the dimensional ice depth is

$$b = 2a\sqrt{\kappa}\ \int_o^t t^{n-1/2}\ f'(\beta)\ dt. \tag{21}$$

Integrating equation (21) by parts (and satisfying equation (4) at $\eta = \beta$) gives

$$b = \frac{4a\sqrt{\kappa}}{2n+1}\left(t^{n+1/2} f_n'(\beta) - \int_o^t t^{n-1}\beta^2 f'(\beta)\,dt + 2a\int_o^t t^{2n-1}\beta\left[f'(\beta)\right]^2 dt\right) \tag{22}$$

$$= \frac{4a\sqrt{\kappa}}{2n+1}\left(t^{n+1/2} f_n'(\beta) - I_1 + 2a\, I_2\right) .$$

Using to the properties of ice on page 44, and the value of $C = 1\,^{\circ}F/(hr)^n$, calculation shows that $a = -.00085$; this immediately reveals the fact that the coefficient for the third term of equation (22) contains a smaller order number, a^2. Therefore, all integrals (including I_2) containing the smaller coefficient will be neglected. To integrate I_1, it is necessary to note that

$$\frac{d\beta}{dt} = \frac{1}{t^{3/2}}\left[at^n f'(\beta) - \frac{\beta}{2}\right] \tag{23}$$

which is obtained directly from the definition of β and equation (20). Using this with

$$f''(\beta) = -2\,\beta\, f'(\beta) , \tag{24}$$

an approximate series solution for (22) may be found.

Dividing the result by $2\sqrt{\kappa t}$ yields the series solution

$$\beta = \frac{2at^n f'(\beta)}{2n+1}\left[1 - \frac{\beta^2 t^{-1/2}}{n} + \frac{\beta^2(\beta^2-1)\,t^{-1}}{n(n-1/2)} - \cdots\right] \tag{25}$$

Assuming the first term is large compared with all the remaining terms (refer to Appendix D), then, the solution for dimensions less ice depth simplifies to

$$\beta = \frac{2a\,t^n fn'(\beta)}{2n+1} \,. \tag{26}$$

Solution (26) may be obtained directly by integrating (20) with respect to time and holding β fixed.

In the case of the Neumann problem, using n = 0 which indicates a temperature step change at the surface, equation (26) reduces to

$$\beta = \left(\frac{CpC}{\sqrt{\pi}\,L}\right)\frac{e^{-\beta^2}}{erf\beta} \tag{27}$$

which shows that the dimensionless ice depth is a constant dependent upon the thermal properties of the frozen region and the surface temperature step change. The ice front progression is therefore proportional to $\sqrt{t}$ for this special case.

Observing the form of equation (27), a useful dimensionless form for time is

$$\tau^n = \frac{4}{\sqrt{\pi}} \, at^n$$

and therefore the explicit solution (26) is written

$$\beta = \frac{\sqrt{\pi}}{2(2n + 1)} \, \tau^n \, f_n'(\beta) \qquad (28)$$

where $f_n'(\beta)$ is obtained from equation (18).

2.3-2 Quadrature Solution

If 2n is not a positive integer, the quadrature method may be used to calculate the ice depth, β. Differentiating (13) and evaluating at β gives

$$f_n'(\beta) = 4nQ'(\beta) - \frac{2}{\sqrt{\pi}} \, \frac{e^{-\beta^2}}{erf\beta} \left[1 + 4nQ(\beta)\right] \qquad (29)$$

where $$Q'(\beta) = e^{-\beta^2} \int_0^{\beta} f_n(\xi) \, e^{\xi^2} \, d\xi .$$

Substituting (29) into (17) and (16), gives the ice front velocity

$$\frac{db}{dt} = \frac{-K\theta_o}{2\rho L \sqrt{\kappa t}} \left[4nQ'(\beta) - \frac{2}{\sqrt{\pi}} \, \frac{e^{-\beta^2}}{erf\beta} \left(1 + 4nQ(\beta)\right)\right] \qquad (30)$$

The dimensionless ice depth, β, is therefore

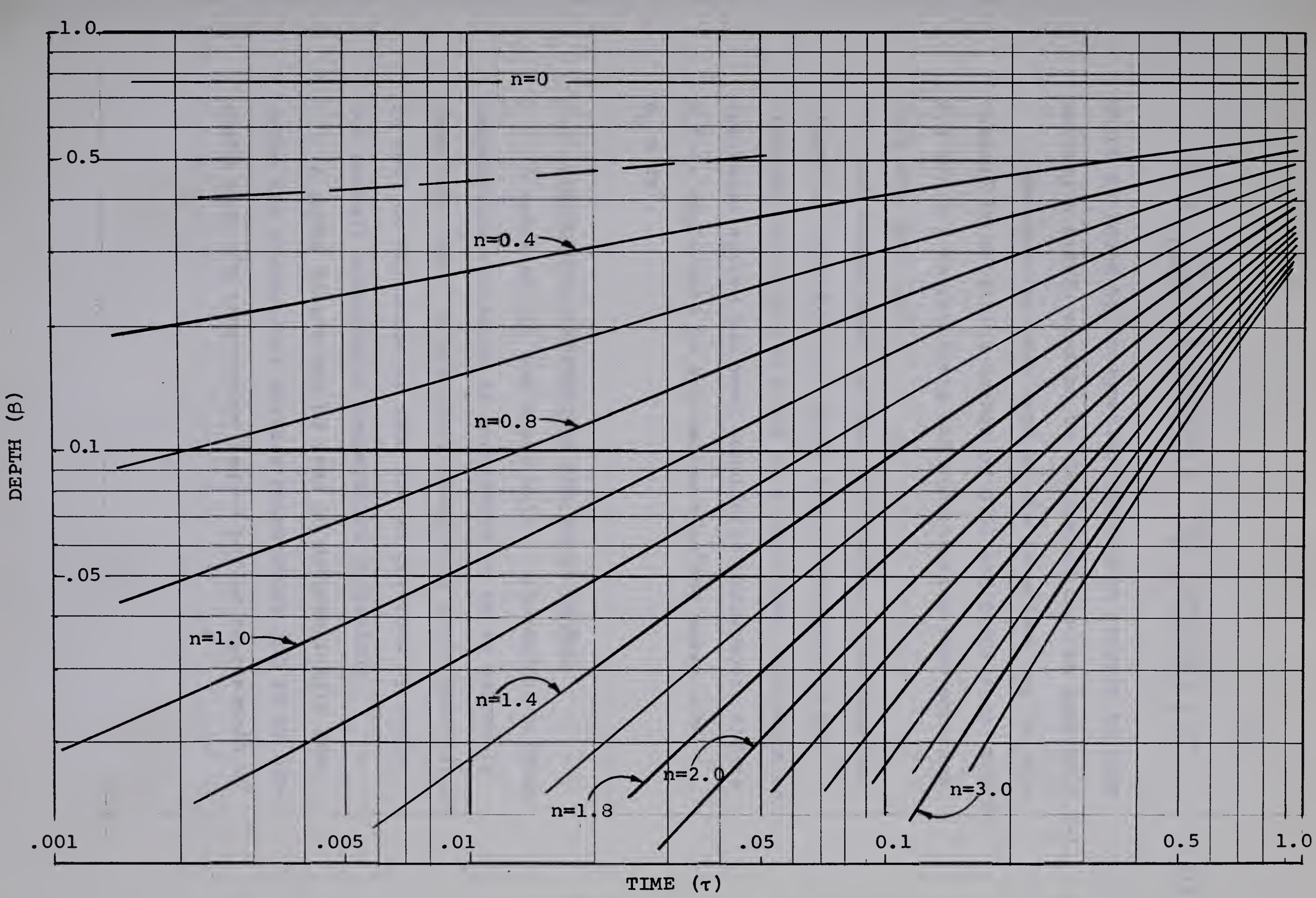

FIG. 2.5 THEORETICAL PROGRESS OF INTERFACE

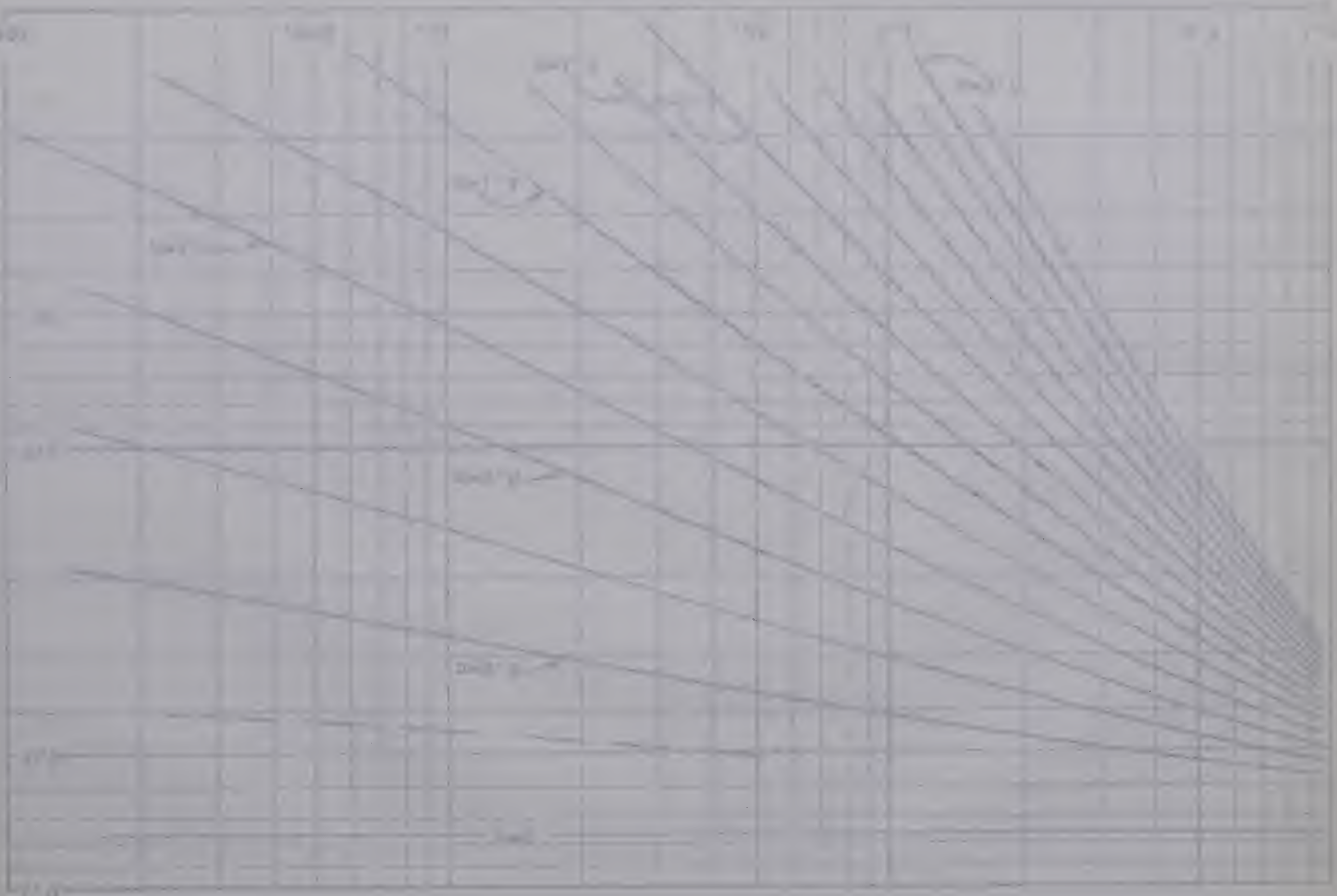

$$\beta = \left[\frac{e^{-\beta^2}}{erf\beta}\left(\frac{1 + 4nQ(\beta)}{2n + 1}\right) - \frac{\sqrt{\pi}}{2}\left(\frac{4nQ'(\beta)}{2n + 1}\right)\right]\tau^n \qquad (31)$$

which is found by integrating (30), with respect to time holding β fixed, similar to the method used in section 2.3-1.

The heat transfer rate at the interface may be calculated by obtaining values of $Q(\beta)$ and $Q'(\beta)$ from figures 2.3 and 2.4 respectively and substituting into equation (30) and then (16).

For convenience, a plot of β versus τ has been included as figure 2.5 in which the convergence to the limiting value of $\beta \approx 0.765$ is illustrated. Although an ice-water system has been considered throughout, figure 2.5 is applicable to any medium changing phase with $\theta_o = Ct^n$.

2.4 SINUSOIDUAL TEMPERATURE AND PHASE CHANGE

A solution for ice depth with a sinusoidual surface temperature variation is considered to be an extremely important case. A practical example is frost penetration in soil or formation of lake ice as governed by daily (or annual) atmospheric temperature variations.

A power series may be used to mathematically describe the sinusoidual surface temperature and it is proposed that the temperature regime may be represented by

$$\theta(\eta) = \sum_{n=0}^{\infty} An\ t^n\ fn(\eta) \ . \qquad (32)$$

The superposition of temperatures should provide a good approximation to the actual temperature regime if CpC/L is of small order. The relative values of this number, for various materials, are shown in Appendix D. If the latent heat of fusion is large (i.e. ice), then the interface will be relatively slow moving. If the specific heat of the solid is relatively small, then surface temperature variations will rapidly vary the temperature regime in the solid region. Thus the superposition method should be quite accurate for large ice depths and/or for a slowly moving interface. In fact, using a periodic boundary temperature, experimental evidence shows that the interface is virtually stationary for a major portion of the cycle (Chapter IV); thus the superposition method should be applicable to this case. Considering the power series

$$\sin \omega t = \omega t - \frac{(\omega t)^3}{3!} + \frac{(\omega t)^5}{5!} - \frac{(\omega t)^7}{7!} + \ldots$$

then, the temperature, in the region $0 < \eta < \beta$, is

$$\theta(\eta) = \theta_m \left[\omega t f_1(\eta) - \frac{(\omega t)^3}{3!} f_3(\eta) + \frac{(\omega t)^5}{5!} f_5(\eta) \ldots \right] \qquad (33)$$

where θ_m is the maximum temperature amplitude. Equation (33)

satisfies the boundary conditions (5). For each half-cycle, the thermal properties will change as shown below:

Range	Properties
$0 < \omega t < \pi$	κ_1, Cp_1, ρ_1 (1 - freezing region)
$\pi < \omega t < 2\pi$	κ_2, Cp_2, ρ_2 (2 - melting region)

For the second half-cycle, the boundary conditions will remain the same and the initial conditions will be nearly the same as those of the first half-cycle. In Chapter IV, experimental evidence will be shown which indicates that the initial domain temperature is virtually zero at the beginning of each cycle and for as many as three cycles.

Applying the energy balance (16), the ice front velocity is

$$\frac{db}{dt} = \frac{-K\theta_m}{2\rho L\sqrt{\kappa t}}\left[\alpha f_1'(\beta) - \frac{\alpha^3}{3!} f_3'(\beta) + \frac{\alpha^5}{5!} f_5(\beta)\ldots\right] \quad (34)$$

where $\alpha = \omega t$ and property subscripts 1 and 2 are deleted. In dimensionless form, the ice depth is

$$\beta = \frac{-Cp\theta_m}{2L}\left[\frac{\alpha f_1'(\beta)}{3} - \frac{\alpha^3}{3!7} f_3'(\beta) + \frac{\alpha^5}{5!11} f_5'(\beta)\ldots\right] \quad (35)$$

Substituting equation (18) appropriately into (35) gives the ice depth as

$$\beta = \frac{Cp\theta_m e^{-\beta^2}}{L}\left[\frac{2}{3}\frac{\alpha}{P_1(\beta) i^2\mathrm{erfc}\,\beta} - \frac{64}{7}\frac{\alpha^3}{P_3(\beta) i^6\mathrm{erfc}\,\beta}\right.$$

$$+ \frac{1024}{11} \quad \frac{\alpha^5}{P_5(\beta) i^{10}\text{erfc } \beta} \quad - \ldots \Big] \tag{36}$$

whereby the necessary functions for $P_n(\beta)$ may be obtained from table 2.1.

For comparison of theory with experimental results, only the first three terms of the series, vis equation (35), are used. For consideration of the half-cycle only, terms beyond the third are small. The first term of the series is the solution for a linear boundary condition. In applying equation (35), a more useful form is

$$\Phi = \frac{-1}{\beta} \left[\frac{\alpha f_1'(\beta)}{3} - \frac{\alpha^3 f_3'(\beta)}{3!7} + \ldots \right] \tag{37}$$

where $\Phi = 2L/Cp\theta_m$. From the computer data, a plot of β versus Φ (reciprocal of temperature) has been included as figure 2.6. The figure indicates that the maximum ice depth increases sharply for values $\Phi < 60$ or alternatively, as θ_m increases. An important criterion* for predicting maximum ice depth is, therefore, θ_m, for a mean temperature at zero datum and for one cycle.

---

* A vast number of field trials in the study of annual frost penetration have indicated that the number of degree-days below freezing per annum, i.e. proportion of area of sinusoidual curve below 32 °F as compared with that above 32 °F, will govern the depth of freezing. The trials indicated that ice depth will increase if the mean is 30 °F and below.

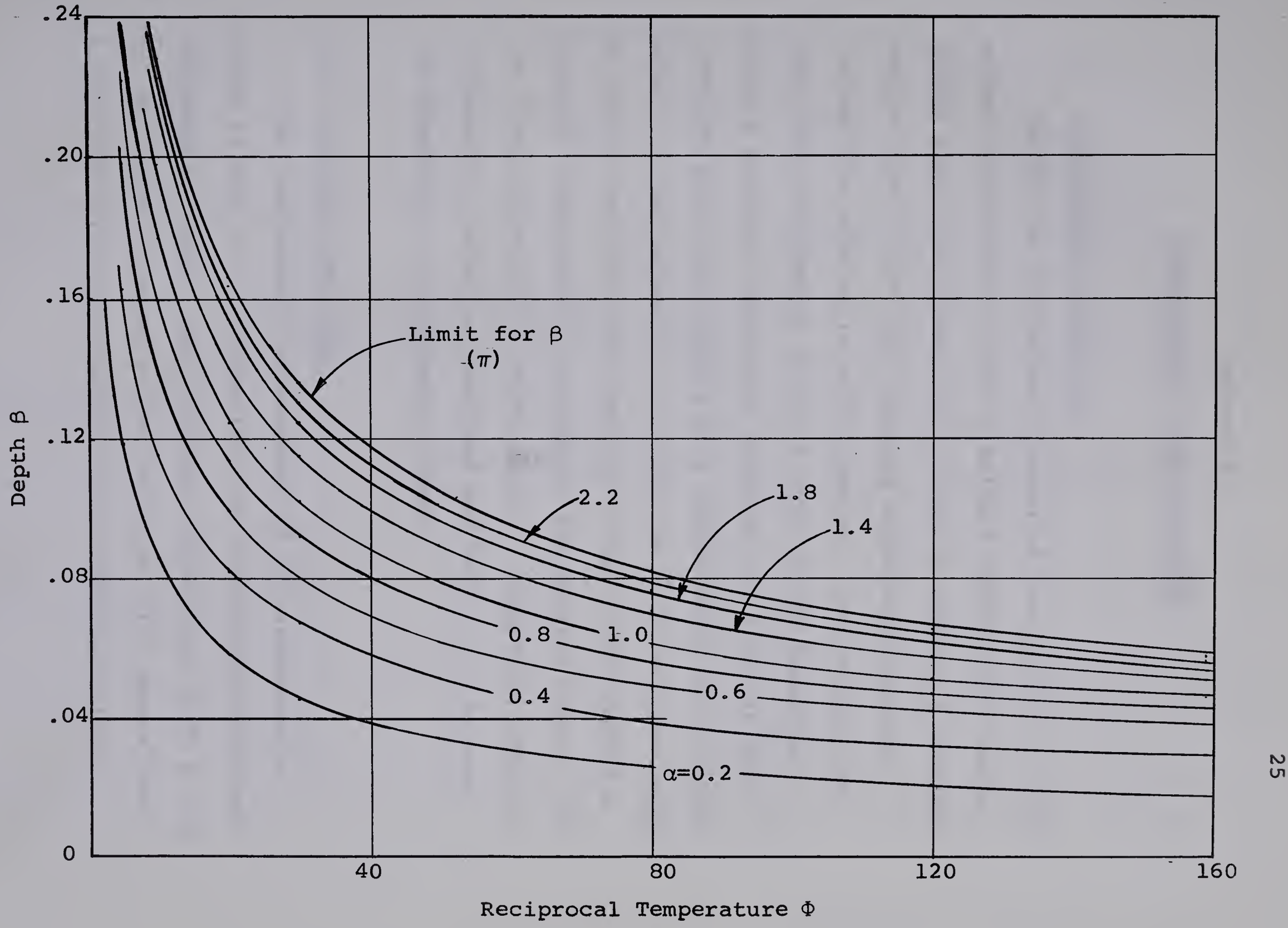

FIG. 2.6 RECIPROCAL TEMPERATURE Φ VERSUS DEPTH β

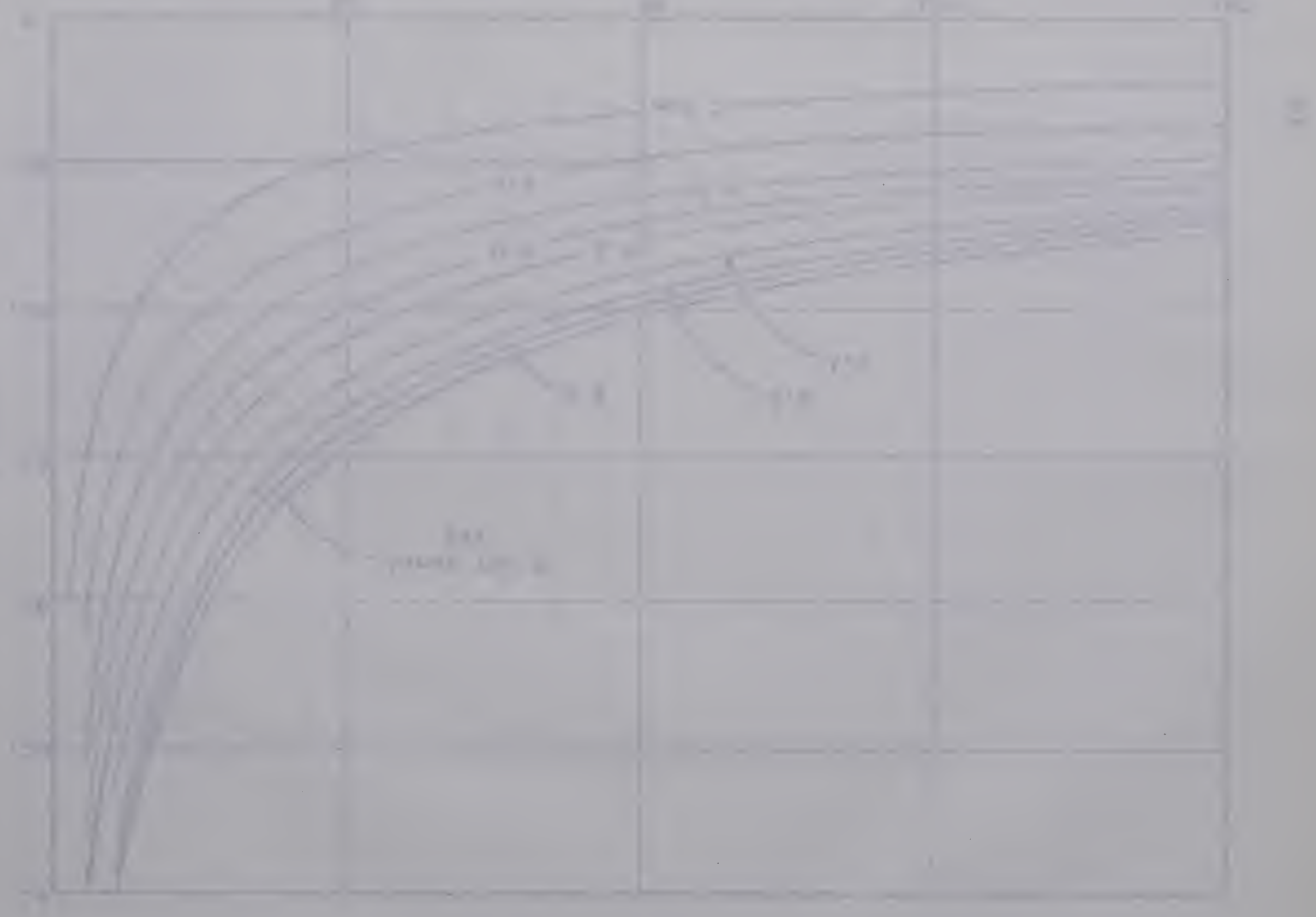

CHAPTER III

EXPERIMENTAL CONSIDERATIONS

3.1 EXPERIMENTAL APPARATUS

During the preliminary design of the apparatus, the primary consideration was to build a device which would freeze water one-dimensionally from an upper flat surface and be able to view the freezing interface laterally through the side walls of the device. The original design was satisfactory for this type of ice formation using a surface temperature starting initially at the freezing point and varying by a simple power law of time. Later, it was necessary to modify the refrigeration jacket by installing electrical heating coils to help impose a periodic temperature variation at the surface plate. In the final phase of the experiments, a completely new refrigeration jacket was designed and built to undertake two-dimensional ice formation tests.

3.1-1 Original Test Cell

The diagrammatic arrangement of the apparatus is shown in fig. 3.1. It consisted of a transparent-walled, rectangular plastic tank (internal dimensions 10.87 x 7.50 x 7.94 inches.) cooled at the top by an 81.5 square inch x 1/8 inch thick copper plate which formed an integral

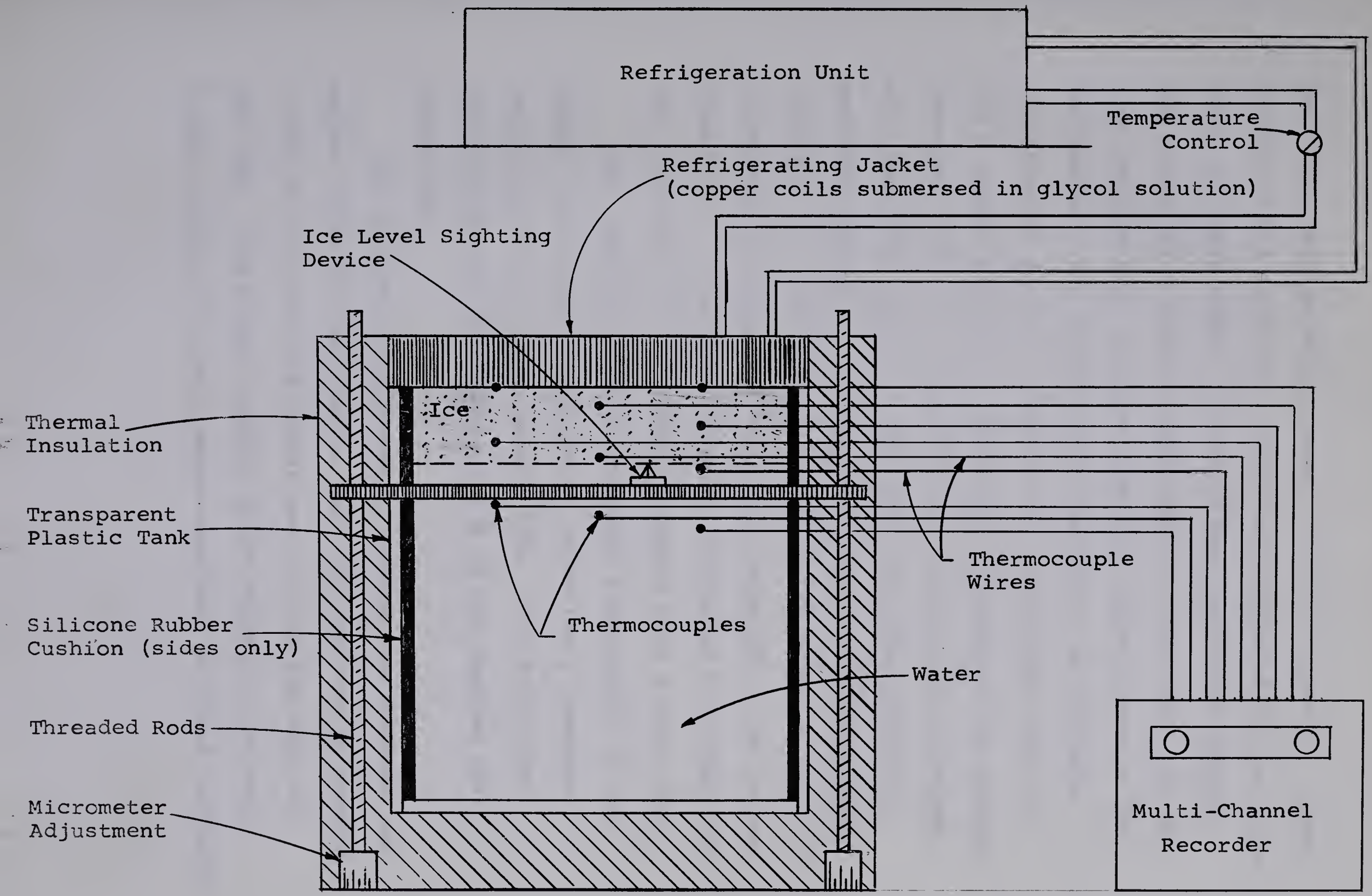

FIG. 3.1 DIAGRAMMATIC ARRANGEMENT OF APPARATUS

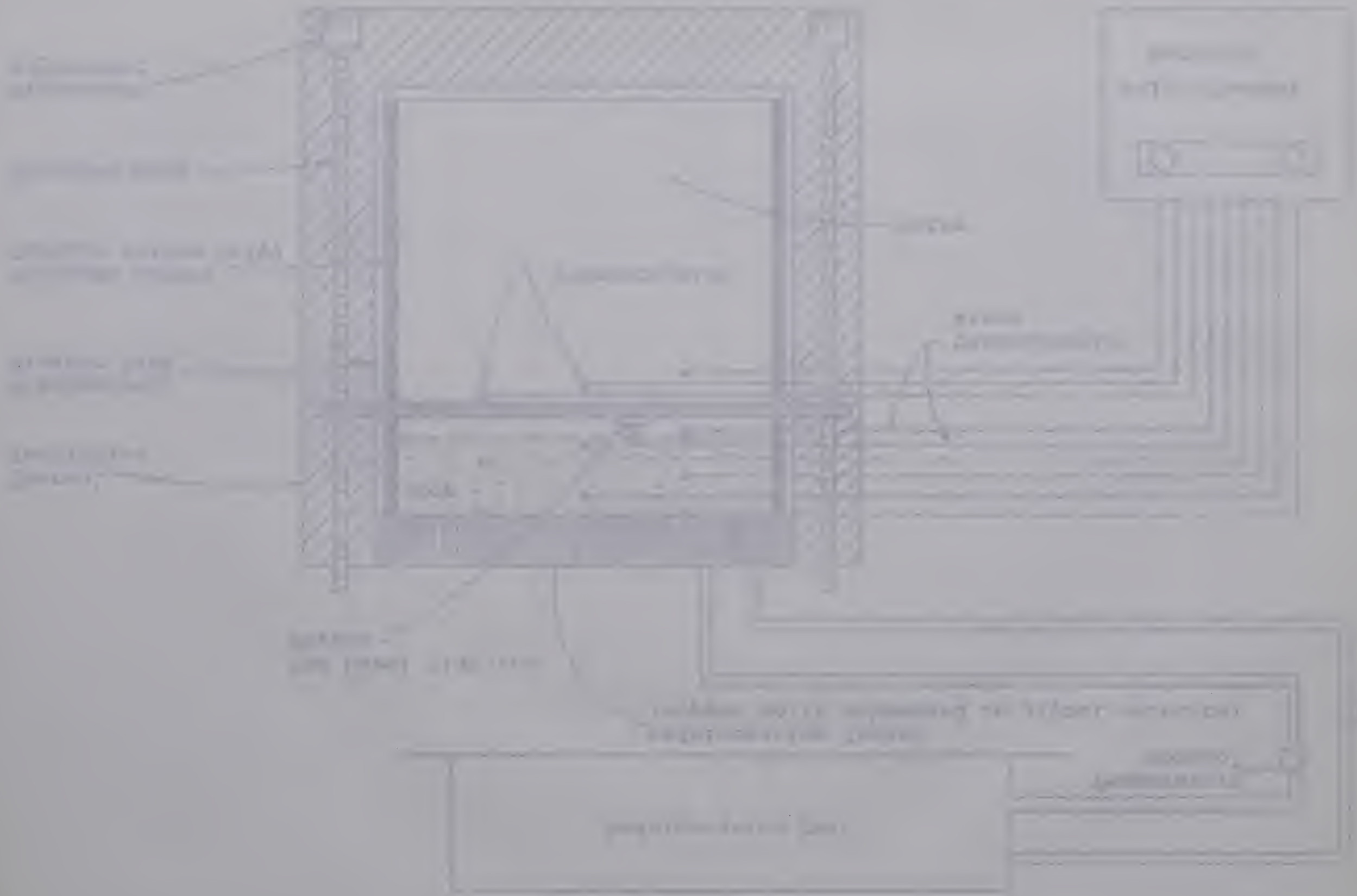

part of a refrigeration jacket. The refrigeration jacket contained 1/4 inch O.D. copper tubing bonded to the copper plate by epoxy resin. Freon 12 was circulated through the tubing by a vapour-compression refrigerator. To provide uniform heat transfer from the copper plate to the refrigerant, the tubing was submerged in an ethylene glycol/water solution capable of temperatures down to -34 °F before freezing. The sides and base of the plastic (Perspex) tank were insulated by 3 inch thick styrofoam with removable panels on the front and rear sides for periodic observation of the ice growth. Silicone rubber cushions were inserted at each side, as shown in fig. 3.1, to reduce the danger of expansion breakage in the lateral direction. To prevent vertical lifting of the copper surface, the water was allowed to expand into a stand pipe.

The temperature of circulating refrigerant in the copper tubing was controlled by adjusting a pressure-regulating valve in the return line. The refrigerant temperature was held within $\pm$ 1 °F of the desired test temperature.

The problem of differential contraction between the copper plate and the plastic tank was overcome by bonding a 1/16 x 1/4 inch hard rubber seal to the top edge of the tank. The copper surface plate rested on the seal. A small amount of highly water-repellent silicone lubricant

was used on the seal. To complete the assembly, four yellow-brass threaded rods were installed near the edge of the plastic tank base and with provision of a 1/2 inch aluminum plate cover on top the refrigeration jacket, the copper surface plate was screwed down onto the seal.

To facilitate removal of air bubbles, a 1/4 inch O.D. overflow tube was incorporated in one corner of the surface plate. Tilting the surface forced the air out through the tube during filling; the tube was clamped shut when all the air was removed. For convenience during filling and draining, the complete test cell was mounted over a laboratory sink as shown in fig. 3.2.

3.2 TEMPERATURE INSTRUMENTATION

Temperatures were measured using eight iron-constantan thermocouples, with a resolution of $\pm$ 0.25 $^{\circ}$F and calibrated at -40 $^{\circ}$F, 0 $^{\circ}$F and 32 $^{\circ}$F with a linear variation between these points. They were housed in Type 316 stainless steel tubes (0.0625 inch O.D. x 0.016 inch wall) located at discrete levels ranging between 0.120 and 1.035 inch below the surface. The tubes were mounted parallel to the upper surface (along isotherms) to reduce conduction losses; they were staggered at various levels in three vertical rows, each row spaced 2-1/2 inches from the other. The tubes afforded good chemical and physical protection to the thermocouples and prevented thermocouple wires from sagging.

Initially, there was some question whether the presence of stainless steel tubes inside the test section would distort the isotherms and create test result errors. However, it was considered that isotherm distortion would be insignificant when taking into account the large dimensions of the test cell as compared with the small size of tubing.

Two additional thermocouples were installed in small diameter holes drilled into the surface plate from the upper side. Temperature measurements from these were averaged to furnish the experimental "surface" temperature.

During preliminary tests, two strip chart recorders were used to record thermocouple temperatures. A high sensitivity single channel Honeywell Electronik 19 recorder was connected to one surface thermocouple to evaluate the maximum "oscillation" amplitude of surface temperature. This was necessary because the time dependent temperature boundary conditions were obtained by approximating the desired function of time with a series of small step changes. For larger step changes, the oscillation was greater. The maximum amplitude of this oscillation was of the same order as the refrigerant temperature variation. A lower sensitivity sixteen channel Brown-Honeywell recorder, with a range of -50 °F to +100 °F

provided a chart record of the remaining nine thermocouples during each run, the circuit of sixteen channels being recorded every 2-1/2 minutes.

3.3 INTERFACE DEPTH MEASUREMENT

To facilitate ice depth measurement, a flat aluminum bar was mounted laterally across the front of the clear plastic test section. Threaded brass rods were installed at each end of the bar which allowed uniform vertical movement by rotating each rod an equal number of turns. Each turn moved the bar vertically 0.020 inch. Scribed micrometer knobs and revolution counters were fitted to the rods. A rifle-sight, with fore and aft vertical adjustments, was mounted in a lateral slot on top of the aluminum bar. The rifle-sight was zeroed on the underside of the surface plate prior to each test and after repeated checks the accuracy of sighting on the surface was found to be $\pm$ 0.002 inch. However, the overall accuracy of the arrangement was considered to be $\pm$ 0.005 inch.

3.4 MODIFICATIONS TO EXPERIMENTAL APPARATUS

3.4-1 Slab Test

A simple addition was made to the test cell to simulate freezing of a shallow lake. The requirement was to provide a finite water layer over a solid substrate and

to use a power law variation of surface temperature. The choice of material for the substrate was styrofoam which provided a near zero heat transfer boundary condition. The styrofoam properties were (approximately):

$$K = 0.02 \quad BTU/hr\ ft\ ^{\circ}F$$

$$C_p = 0.2 \quad BTU/lb_m\ ^{\circ}F$$

$$\rho = 1.9 \quad lb_m/ft^3$$

$$\kappa = 0.0525 \quad ft^2/hr \text{ (calculated)}$$

The substrate was pressed firmly into the lower section of the plastic tank and the remaining volume was filled with tap water to a depth of 1 inch in preparation for the test.

3.4-2 Sinusoidual Temperature Tests

After the initial set of tests, using the simple power law variation in surface temperature, a periodic temperature variation over three cycles was attempted. External heat lamps were required to raise the surface temperature to the necessary degree above freezing prior to returning to below freezing in each cycle. For a second test, an electrical heating wire, wound over two 3/4 inch O.D. Teflon rods, was submerged in the glycol solution in the refrigeration jacket. This heater replaced the cumbersome heat lamp arrangement. Electrical power to the heating element was controlled by a Variac unit.

3.4-3 Two-Dimensional Tests

With completion of the one-dimensional tests, a revised refrigeration jacket was manufactured and mounted onto the original plastic tank for a study of two dimensional ice formation. For this particular study, extensive modifications were required. The complete two-dimensional test apparatus is shown in fig. 3.2.

The aim of the test was to locate the steady state ice profile under the edge of a surface held at a uniform temperature below freezing and with the adjacent surface held at a uniform temperature above freezing.

The revised jacket consisted of two copper plate surfaces separated by an insulation of 1/4 inch asbestos board. The yellow-brass side walls of the jacket were identical to those used in the original test cell. Identical copper cooling coils were mounted on each surface plate and connected in parallel to the refrigerator with a shut-off valve incorporated to control Freon 12 flow to the right-half coil. An important additional feature was the inlet/outlet ports in the right half of the jacket for circulation of an externally heated glycol/water solution for maintaining a uniform temperature above freezing.

Five iron-constantan thermocouples were installed in the jacket, two on the cooled surface, one centered

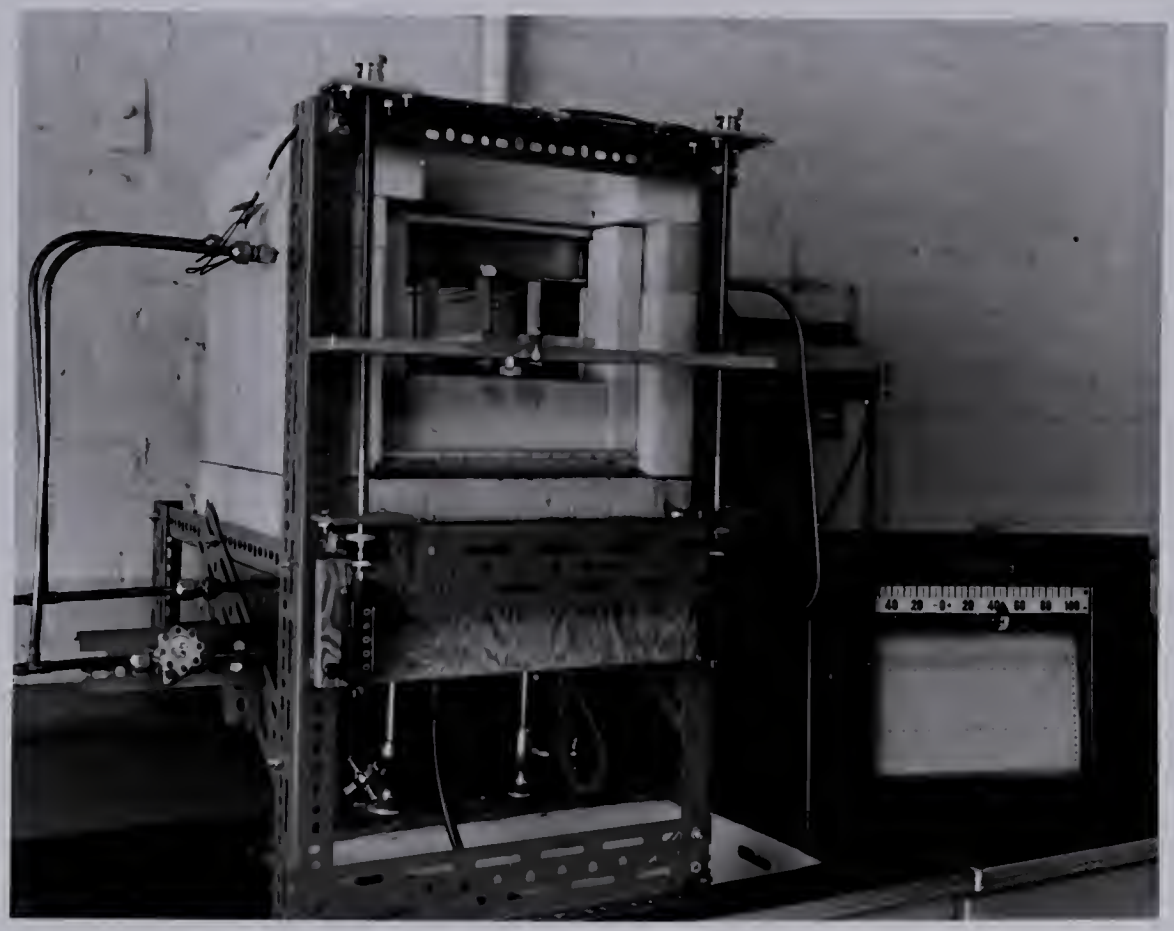

FIG. 3.2 VIEW OF APPARATUS FOR
TWO-DIMENSIONAL EXPERIMENTS

in the asbestos board, and two on the heated surface.

3.5 EXPERIMENTAL METHOD

The analytic model for the power law variation outlined in Chapter II was applicable only to the case when the water was initially at a temperature of 32 °F. Consequently, prior to each test run, the water was cooled from room temperature to a point when the temperature profile was steady and as close to the zero datum as possible. This required approximately 3 hours, at which time the lower thermocouple in the water registered a steady 35-36 °F which was considered to be the limiting case for the apparatus with only 3 inches of styrofoam insulation. The initial departure from zero datum as described above was considered as a condition of "superheat".

3.5-1 Temporal Origin and Supercooling

During the initial power law tests, it was discovered that pronounced supercooling of the water occurred. This was a departure from the theoretical requirement for an initial temperature at zero datum. The difficulty was surmounted, in subsequent power law tests, by producing a thin layer of ice on the surface and then allowing thaw-back until only an extremely thin film of ice was visible on the surface. The test run proper was then started from this point.

Even with precautions to overcome the supercooling effect, the temporal origin of each test run was difficult to fix. To provide a uniform basis for comparison of experiment with the analytic model, the temporal origin was considered to be a time point found by rearward extrapolation of the surface test temperatures to 32 °F. Since thermocouple temperatures were measured over a 2-1/2 minute cycle and all tests were more than one hour duration, the extrapolation was sufficiently accurate to establish the temporal origin.

3.5-2 Typical Test Procedure

Prior to each test, additional water was forced into the enclosed test cell to remove air bubbles which accumulated at the surface plate between tests. The bulk of the water was then cooled for several hours to near 32 °F. Following this, a thin ice layer was produced by quickly reducing the surface temperature below the freezing point. The surface temperature was then reset to 32 °F and thawback allowed as described previously. During thawback, the ice depth measuring device was "zeroed" on the surface plate by removing the insulated observation panels. The temperature recorders were turned on and at the "critical" moment of thawback, the desired surface temperature variation was initiated. Temperature measurements

were continuous and automatic throughout test runs whereas ice depth measurements were on a periodic inspection basis.

3.6 SUPPLEMENTARY SUPERCOOLING EXPERIMENTS

Another set of experiments were undertaken to find a relation between the surface cooling rate and supercooled time period required for ice to form. As in previous experiments, tap water was used. The apparatus was a 3M Brand Thermoelectric Cooler Model 11 B; it consisted of a 0.32 cubic inch cylindrical cavity insulated with styrofoam and cooled by thermoelectric modules. Thermocouples and an electrical power source were installed for the tests. By comparison, the volume of the freezing cell used in the main experiments was over 2,000 times larger than the thermoelectric cell.

A set of 10 test runs were conducted with the thermoelectric unit. Results were compared with three prior tests on the large freezing cell.

CHAPTER IV

DISCUSSION OF RESULTS

4.1 SUPERCOOLING

One of the first problems encountered in the experimental programme was that of water supercooling near the surface prior to formation of ice. During initial tests, water temperatures as low as 22 °F were recorded before crystallization. Numerous ice spikes or "spicules" propagated rapidly downward into the water; in one test, spicules penetrated 3/8 inch within a period of 30 seconds. Following their formation, the lower ends of the spicules melted back uniformly and gradually degenerated into a thinner but homogeneous layer of ice. From this point, a plane ice-water interface propagated.

A typical temperature record (n = 1.0 and C = 25.0 °F/hr.) indicating supercooling is shown in fig. 4.1 and clearly shows a metastable period followed by a very rapid surface temperature increase. This is compared with another test (n = 0.71 and C = 25.0 $°F/hr^{0.71}$) where ice was formed initially and melted back to a thin film prior to the test run. Fig. 4.2 illustrates the steps (a) to (d) which are believed to occur during supercooling and subsequent ice formation.

A second test (n = 1.0 and C = 25.0 °F/hr) was carried

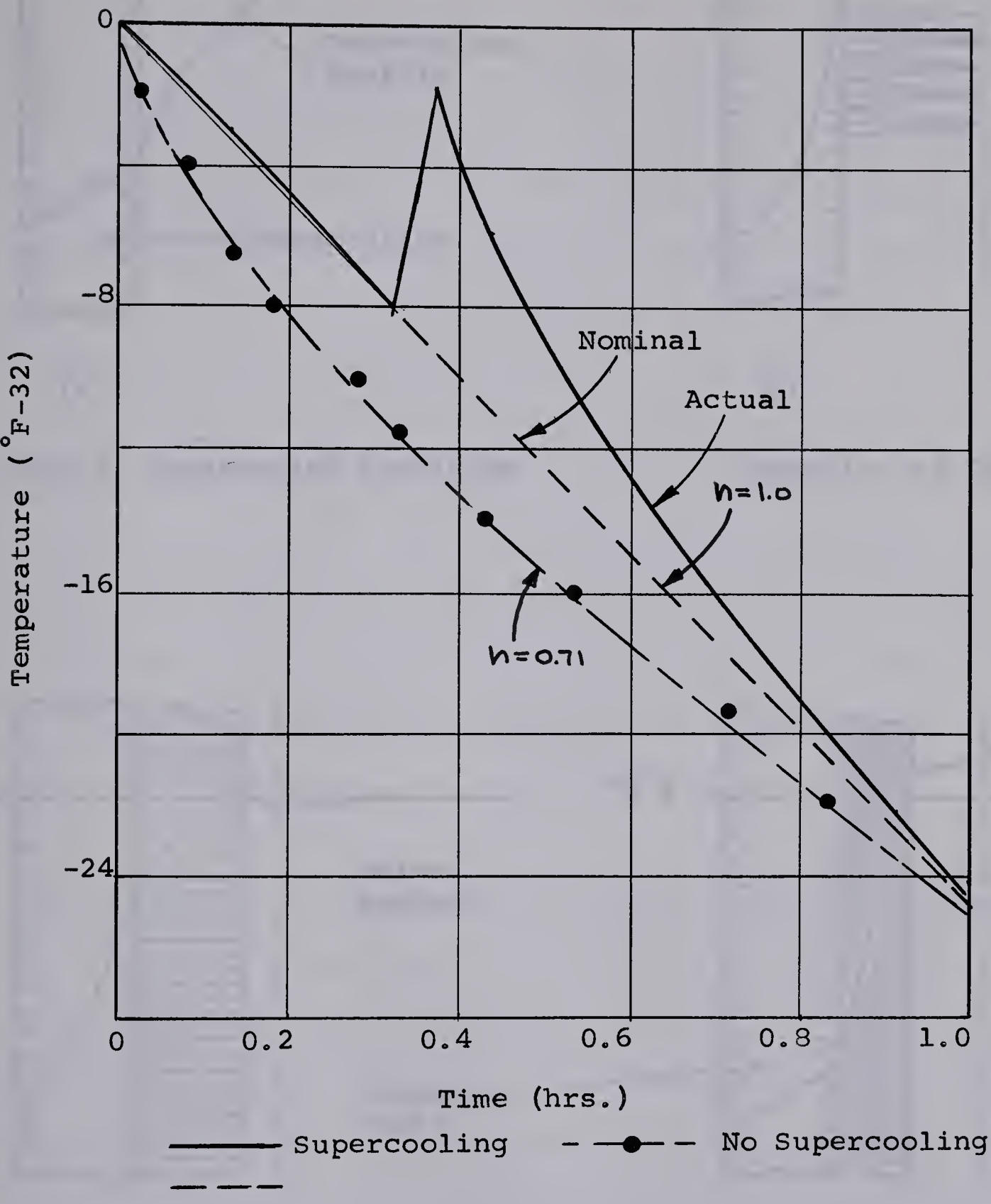

FIG.4.1 TYPICAL SURFACE TEMPERATURE RECORDS

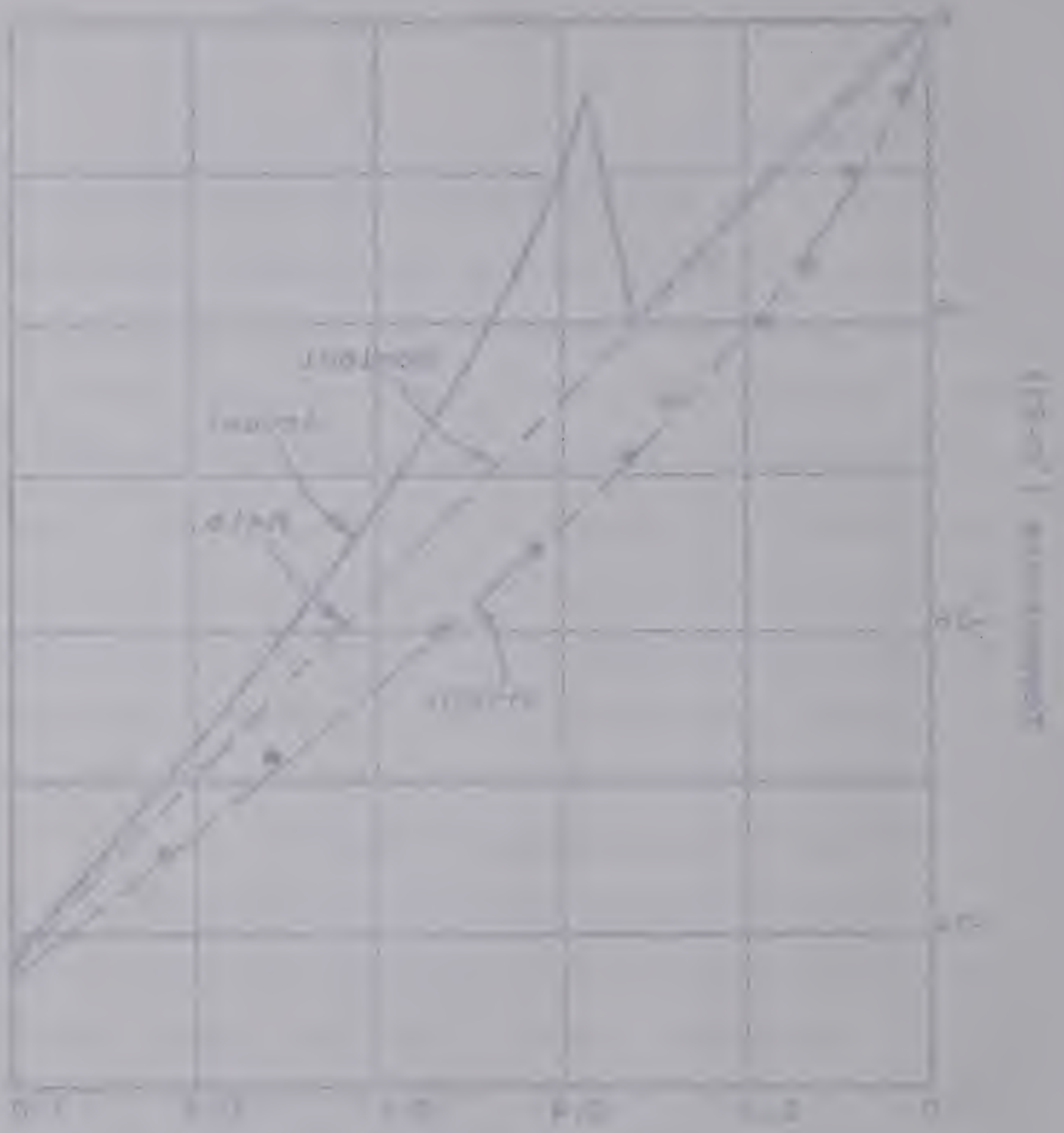

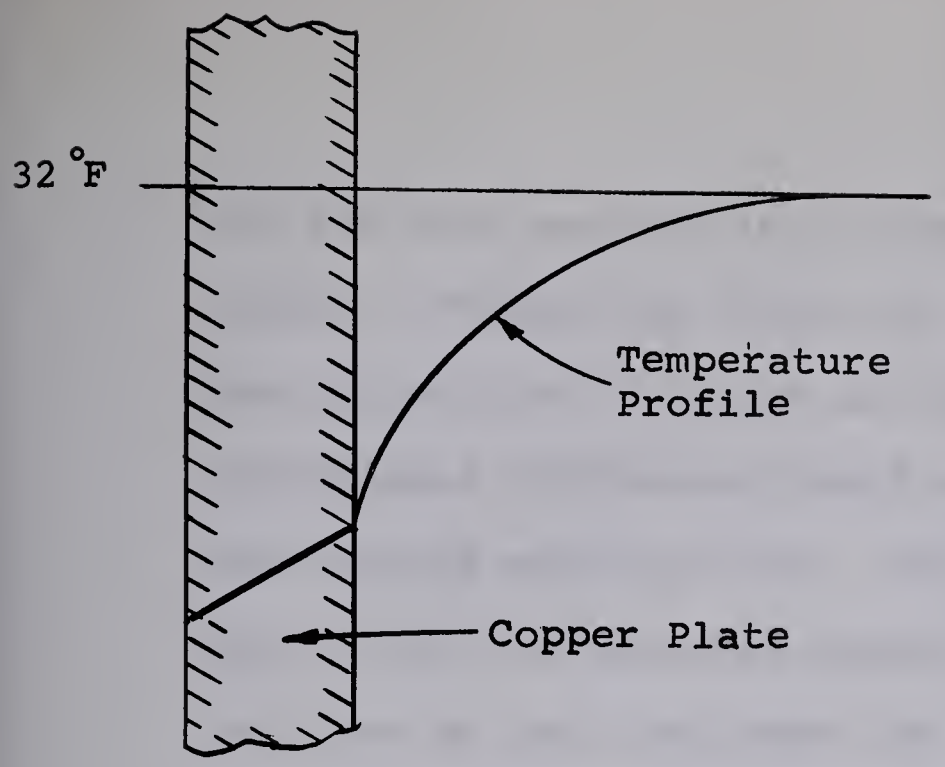

(a)

Initial Supercooled Condition

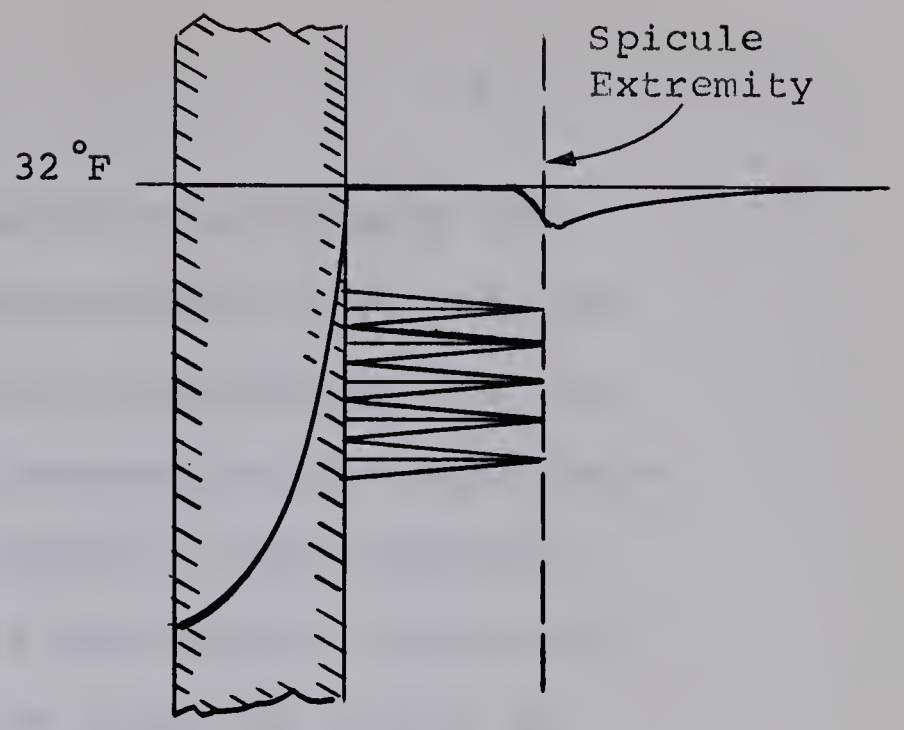

(b)

Formation of Ice Spicules

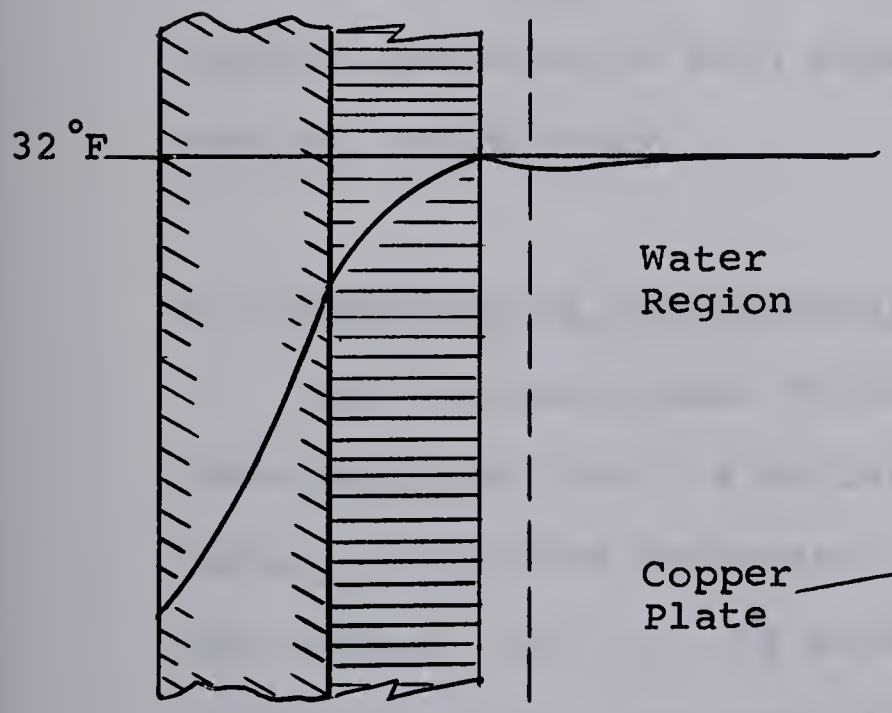

(c)

Formation of Ice Layer

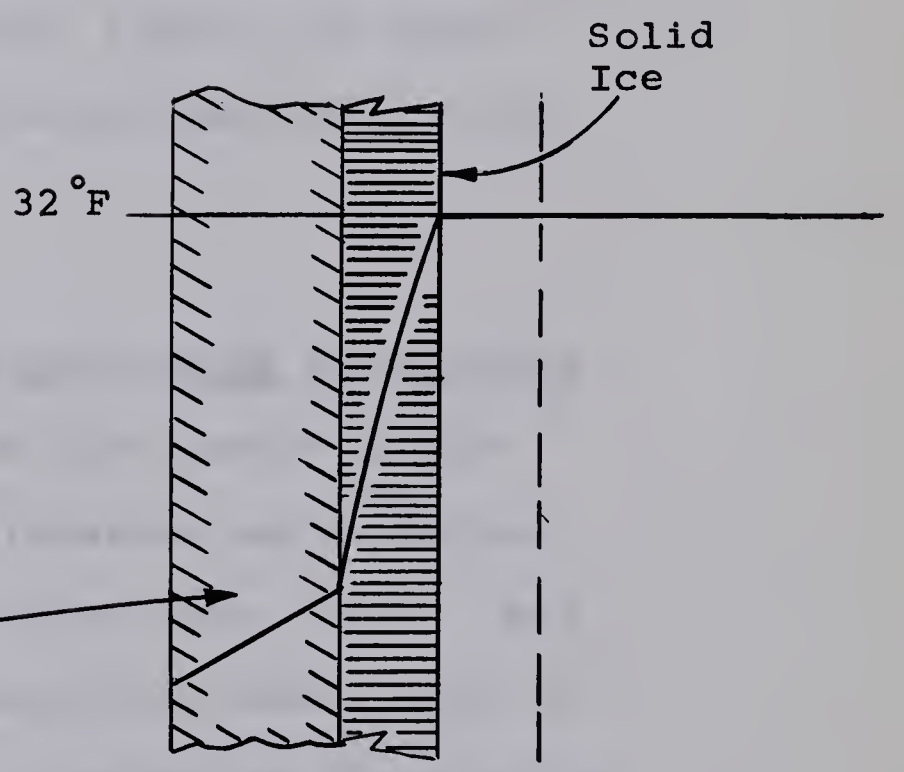

(d)

Final Stable Condition

FIG. 4.2 TEMPERATURE PROFILES DURING SUPERCOOLING AND ICE FORMATION

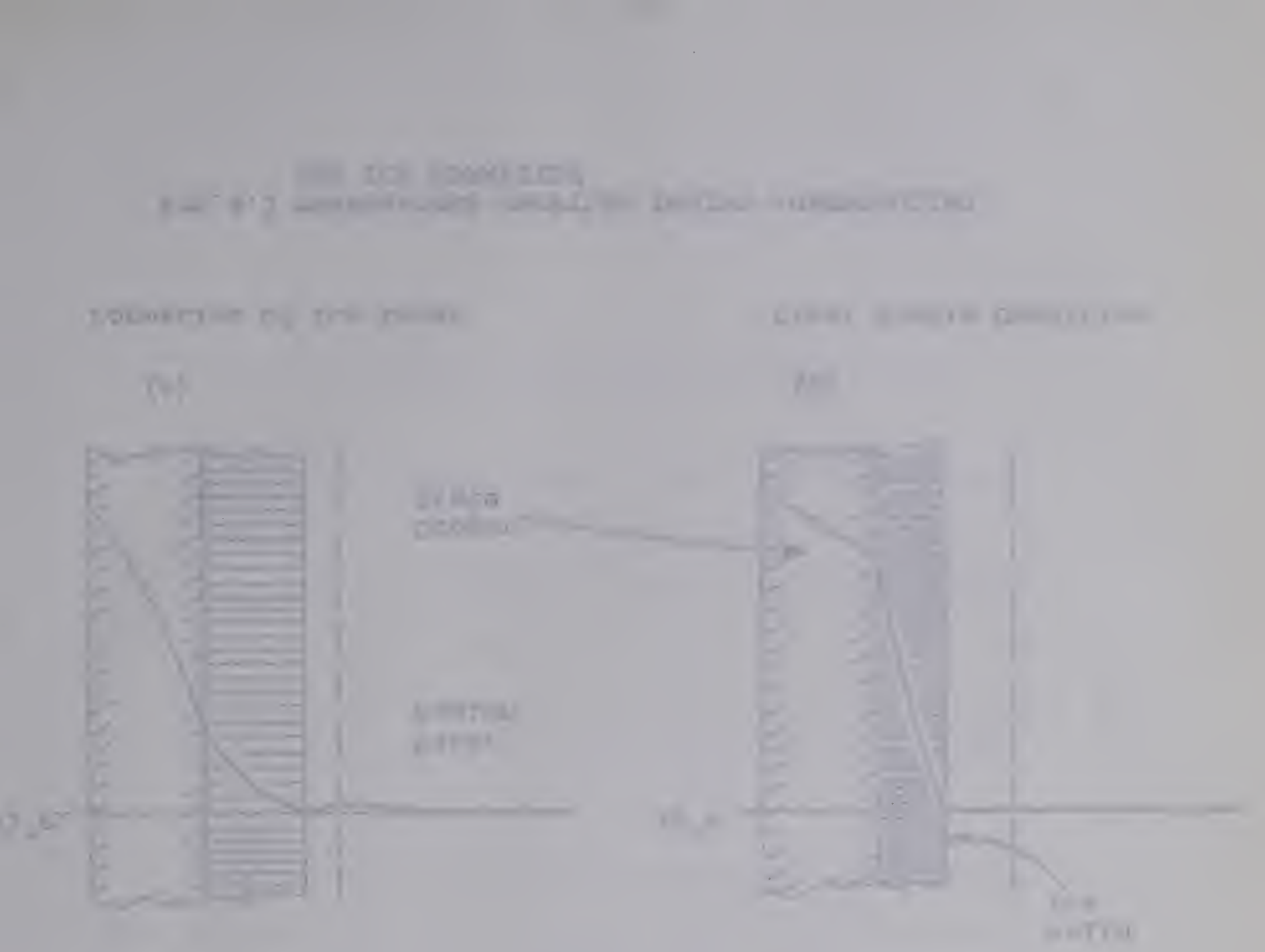

out but with supercooling eliminated as previously described. Within the limits of experimental error and one hour after the time zero as defined in section 3.5-1, no appreciable difference could be measured in ice depth with and without supercooling. This leads to the important point that the temporal origin in experiments should not be taken as the time when ice just forms but rather as the time defined in section 3.5-1. For longer time periods, after supercooling with subsequent ice formation, the analytic solution should provide an accurate prediction of ice depth. Fig. 4.1 further substantiates the idea that supercooling does not cause a serious departure from the analytic model; for longer times, the actual surface temperature with supercooling converged to the nominal temperature.

4.1-1 Results of Supplementary Supercooling Experiments

For the particular volume of test cavity in the thermoelectric unit, a definite relation was found between the surface temperature cooling rate, $d\theta_o/dt$, and the maximum time, t_c, of supercooling of water prior to crystallization. The empirical relation was found to be

$$\frac{d\theta_o}{dt} = 1.22\ t_c^{2.54} .$$

Considering supercooling and the particular linear surface temperature shown in fig. 4.1, the empirical relation predicts that $t_c = 0.304$ hr. using $\theta_o = Ct^n$ where $n = 1.0$; this agrees well with the time of crystallization in fig. 4.1. In more general terms, the maximum time (using the above surface temperature) is

$$t_c = \left[\frac{nC}{1.22}\right]^{\frac{1}{3.54-n}}$$

which points out the possibility of no ice forming when $n = 3.54$ and thus $t_c \rightarrow \infty$.

During the small cavity tests, the sudden temperature rise associated with formation of stable ice was constant at $12.75 \pm 0.5\,^{\circ}F$ for all test runs regardless of the degree of supercooling. This was contrasted with a typical surface temperature rise of 5 to $7\,^{\circ}F$ in the larger apparatus. The difference stems from the difference in dimensions of the two systems and the volume of ice formed. Initially, it was thought that stable ice filled the smaller unit almost instantly with no apparent thawback. However, the latent heat released was calculated to be only .015 BTU whereas to fill the unit completely with ice would require a release of 0.171 BTU. A period of up to 3 minutes was required for stable ice to form, after thawback, in the larger unit.

The degree of supercooling encountered in the

supplementary experiments ranged as low as 21°F below the normal freezing temperature using ordinary tap water. Turnbull [13] has indicated that under special conditions, very pure water can be supercooled to as low as -40°F without crystallizing into ice.

4.2 INITIAL ICE FORMATION

From the beginning of the test programme, when difficulty was encountered in trying to establish a criterion for temporal origin, a routine was formed to observe the initial ice formation. These observations revealed that a small speck of ice (possibly several actual crystals) would form on the surface plate at a random point. Shortly thereafter, similar specks would form at other points. Almost immediately a crystal speck formed, additional crystals would attach themselves to it fanning out quickly only in a radial horizontal direction along the plate surface. There appeared to be no appreciable crystal growth in the vertical direction until the complete plate surface was covered with an initial thin film of ice crystals.

4.3 RESULTS USING POWER LAW SURFACE TEMPERATURE

4.3-1 Ice Depth

Visual studies of the ice-water interface showed it to be planar, thus implying that the ice crystal growth on the interface proceeded uniformly in a vertical direction. Within the limits of accuracy of the measuring device, it was estimated that departure from flatness was of the order of 0.01 inches. It is uncertain as to how the growth proceeded immediately adjacent to the transparent walls. Removing the observation panels during depth measurement periods caused thawback in this region but allowed accurate determination of the ice depth over the main interface. The estimated thawback adjacent to the walls was usually about 0.1 inch but this was small compared with the total interface area of 81.5 square inches. This suggests that one-dimensional studies could be executed readily with a much smaller surface area and volume of water.

Theoretical and experimental results for the variation of interface depth with time are shown in fig. 4.3 in dimensional form. They are calculated on the assumption that the thermal properties of ice (over the temperature range of $-20\,^{\circ}F$ to $+32\,^{\circ}F$) are constant at:

$$K = 1.4 \text{ BTU/hr ft } ^{\circ}F$$

$$\rho = 57 \text{ lb}_m/\text{ft}^3$$

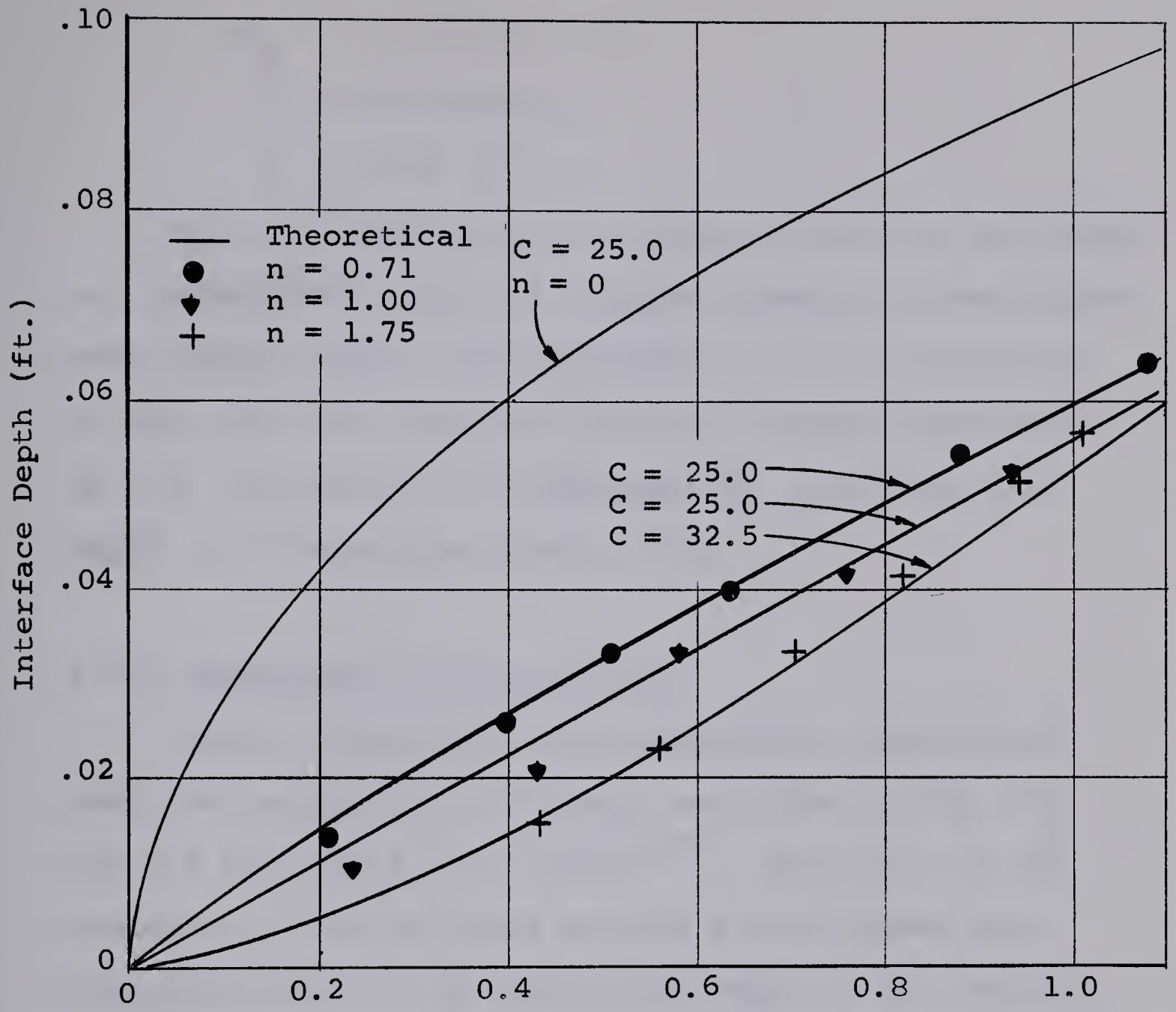

FIG. 4.3 INTERFACE DEPTH VERSUS TIME (POWER LAW)

$$c_p = 0.49 \text{ BTU/lb}_m {}^\circ\text{F}$$

$$L = 144 \text{ BTU/lb}_m$$

$$\kappa = 0.05 \text{ ft}^2/\text{hr}$$

Fig. 4.3 illustrates the effect of varying the boundary temperature index and indicates generally good agreement between theory and experiment. It is interesting to note the large departure from the Neumann Solution ($n = 0$) indicating its inadequacy for predicting ice depth in circumstances where $n \neq 0$.

4.3-2 Temperature Profile In Ice

Typical theoretical and experimental temperature profiles, within the ice layer, are shown in fig. 4.4 for $n = 0.71$ and $C = 25.0\ ^\circ\text{F/hr}^{0.71}$. The value of the constant, C, may be found quickly for any power law variation since it is numerically equal to the temperature reduction below 32 °F (zero datum) when the time, t, is equal to 1 hour. Good agreement with the theoretical temperature profile is evident. Any discrepancy between the theoretical and experimental ice depth may be attributed to three factors: (1) the choice of temporal origin, (2) the uncertainty in the choice of thermal properties (especially considering a 40 °F temperature variation within the ice layer) and, (3) the degree of superheat within the liquid domain. Fig. 4.4 confirms

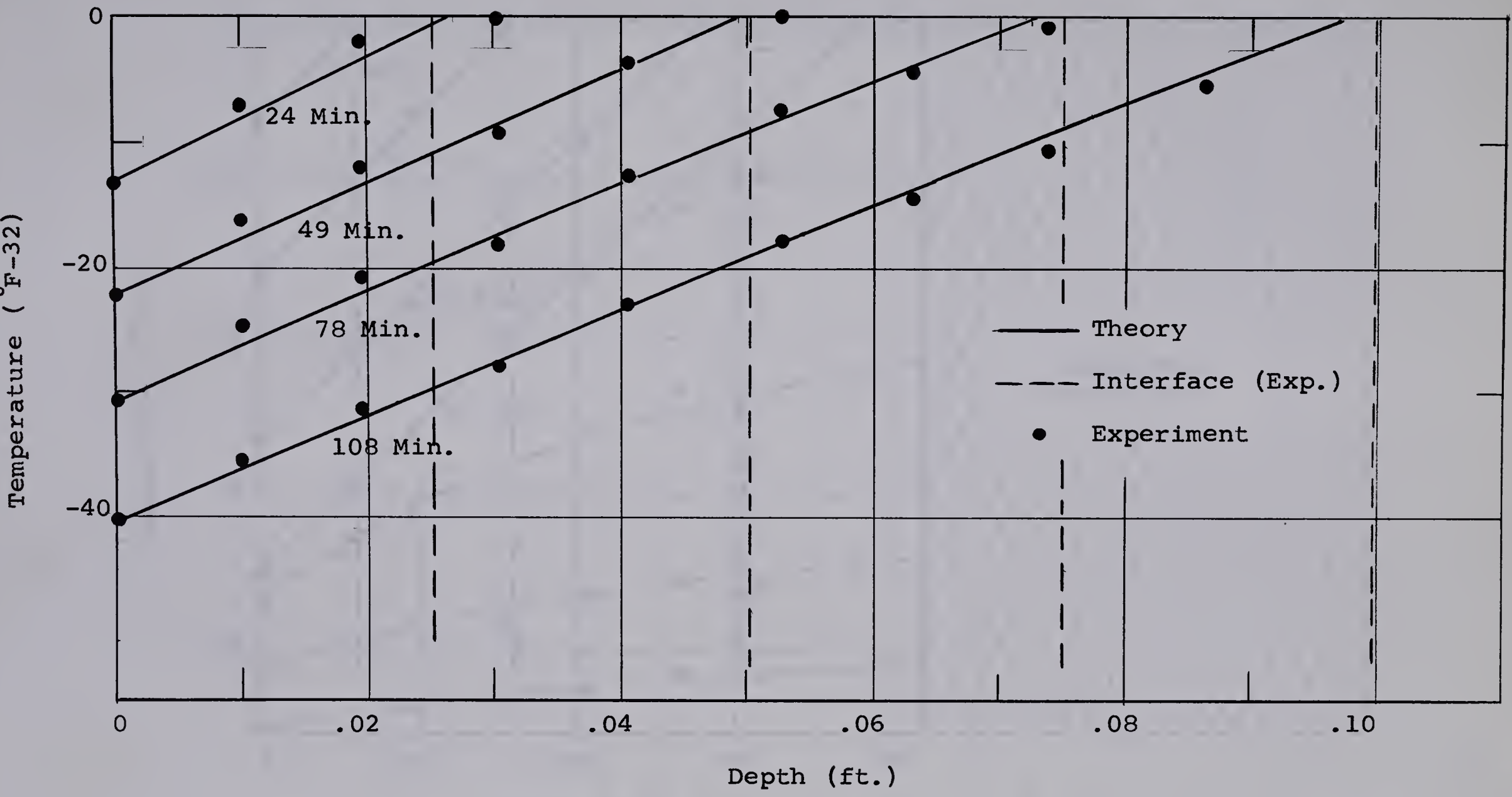

Semi-Infinite Domain (n = 0.71 C = 25.0)

FIG. 4.4 VARIATION OF TEMPERATURE WITH DEPTH (POWER LAW)

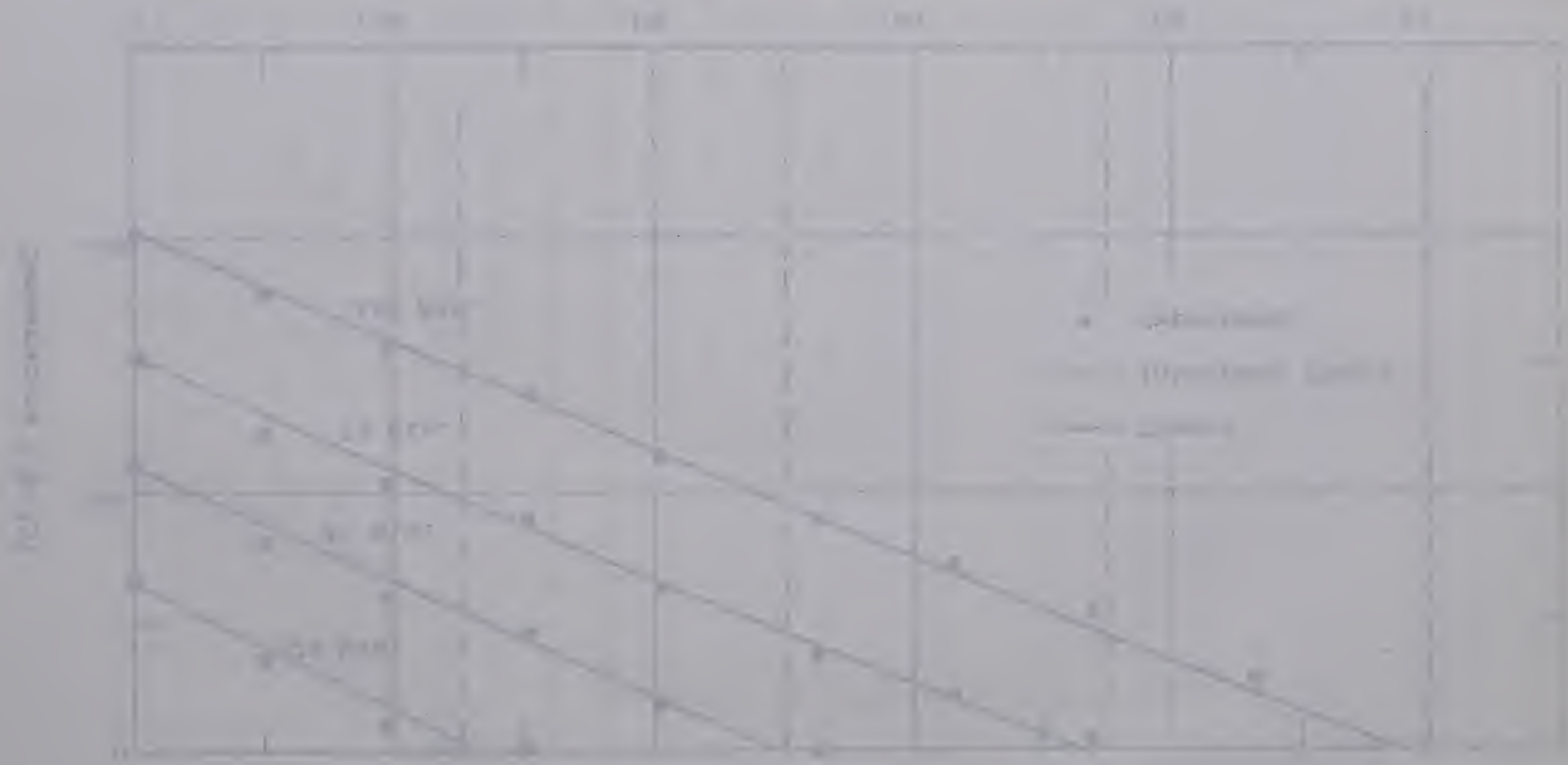

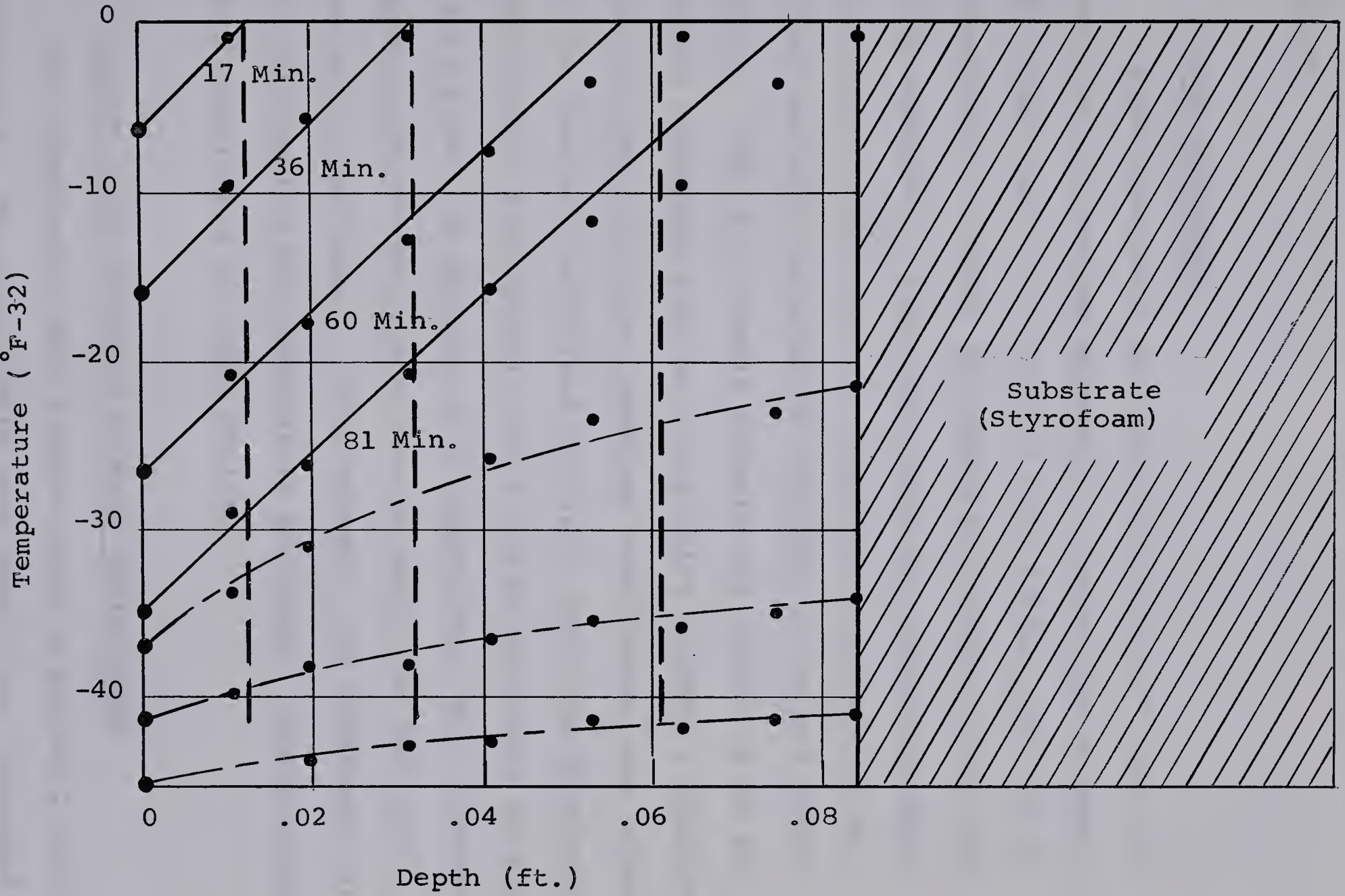

Slab Domain (n = 1.0 C = 27.0)

FIG. 4.5 VARIATION OF TEMPERATURE WITH DEPTH

that the temperature profile is almost linear within the ice.

4.3-3 Slab Experiment

A slab experiment was undertaken with 1" depth of water over a styrofoam substrate. Comparison is made with theory, for n = 1.0 and C = 27.0 °F/hr, only up to thetime when the water is completely frozen to the top of the substrate. After that time the problem becomes one of pure conduction in a stratified medium with an initial non-zero temperature distribution in the upper stratum. Fig. 4.5 clearly reveals the effect of an insulating substrate such as could exist beneath a shallow lake; it shows that the interface accelerates* upon approaching the insulated substrate and also, that the theoretical prediction is satisfactory until 3/4 of the water is frozen. At this time, the absence of a latent heat "sink" causes a pronounced change in the rate at which the bulk ice temperature decreases. Unfortunately, the substrate was not instrumented for temperature and hence, temperatures are not available for that region.

4.4 RESULTS USING PERIODIC SURFACE TEMPERATURE

Two experiments were tackled using a periodic surface temperature. The approximate test conditions, averaged

---

* Refer to Lightfoot [4].

over three complete cycles, were:

Test No.	Temperature Amplitudes	Temperature Mean	ω Radians/hr
1	$\pm$ 8 °F	+ 34 °F	π
2	$\pm$ 19 °F	+ 33 °F	π

For theoretical comparison, fig. 2.6 is used; it is based on a sinusoidual temperature symmetrical about a mean of +32 °F. Fig. 4.6 compares the actual surface temperature with the desired sinusoidual temperature for test no. 2. Test no. 2 was considered more useful for comparison because the ice depth measurements were more accurately done than those of test no. 1.

4.4-1 Ice Depth For Periodic Case

Following the first complete cycle of freezing, a thin layer of ice remained below the surface. However, during test no. 1, no provision was made in the tank to hold the layer at the level where it formed and consequently, it disintegrated easily after melting back to 1/16 inch thickness; this resulted in broken ice sheets floating to the top of the tank. For test no. 2, the problem was overcome by installing four 1/8 inch threaded, stainless steel rods mounted vertically inside the test tank to provide anchorage for the ice layer formed. The shape

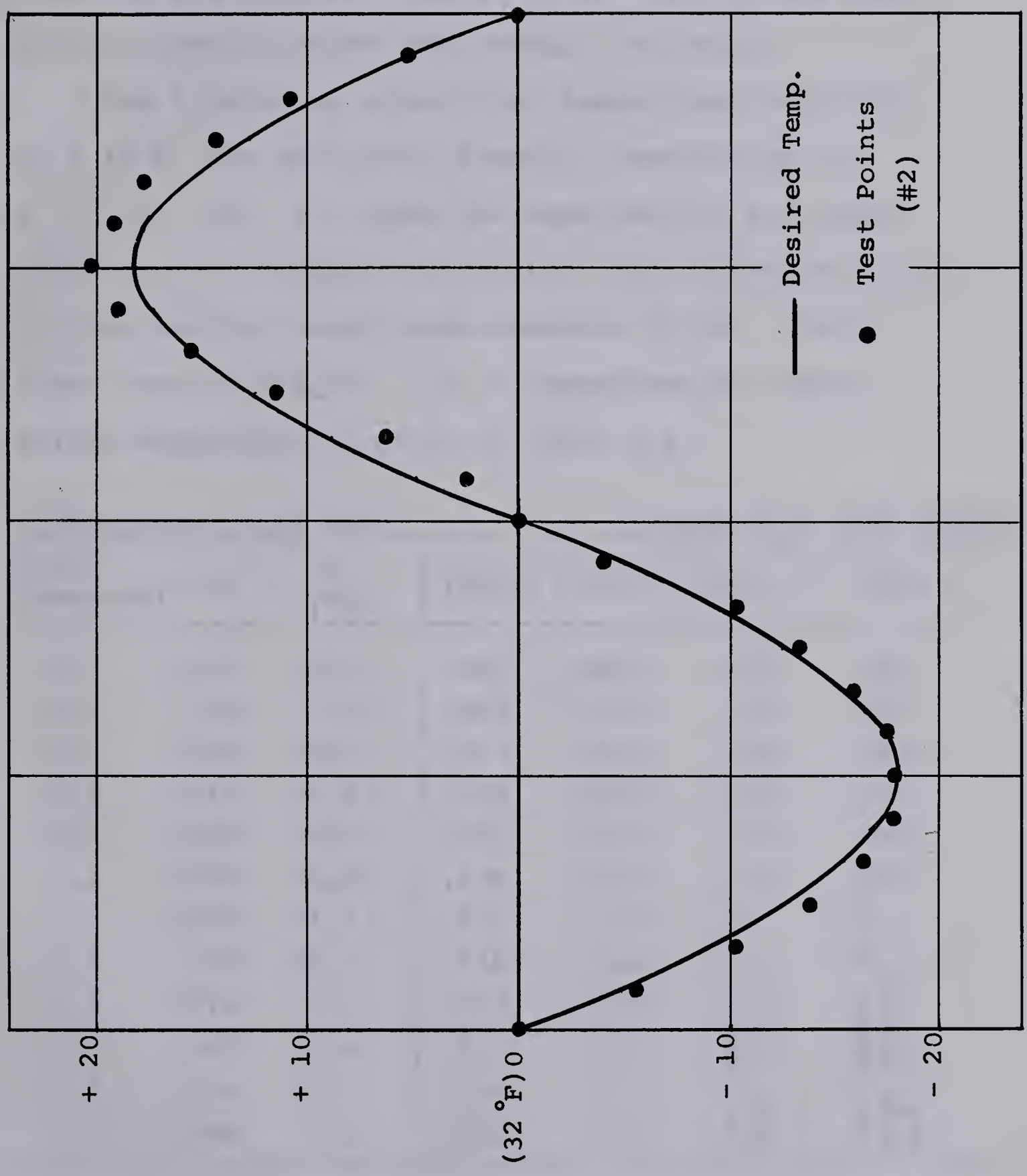

FIG. 4.6 SURFACE TEMPERATURE FOR PERIODIC CASE

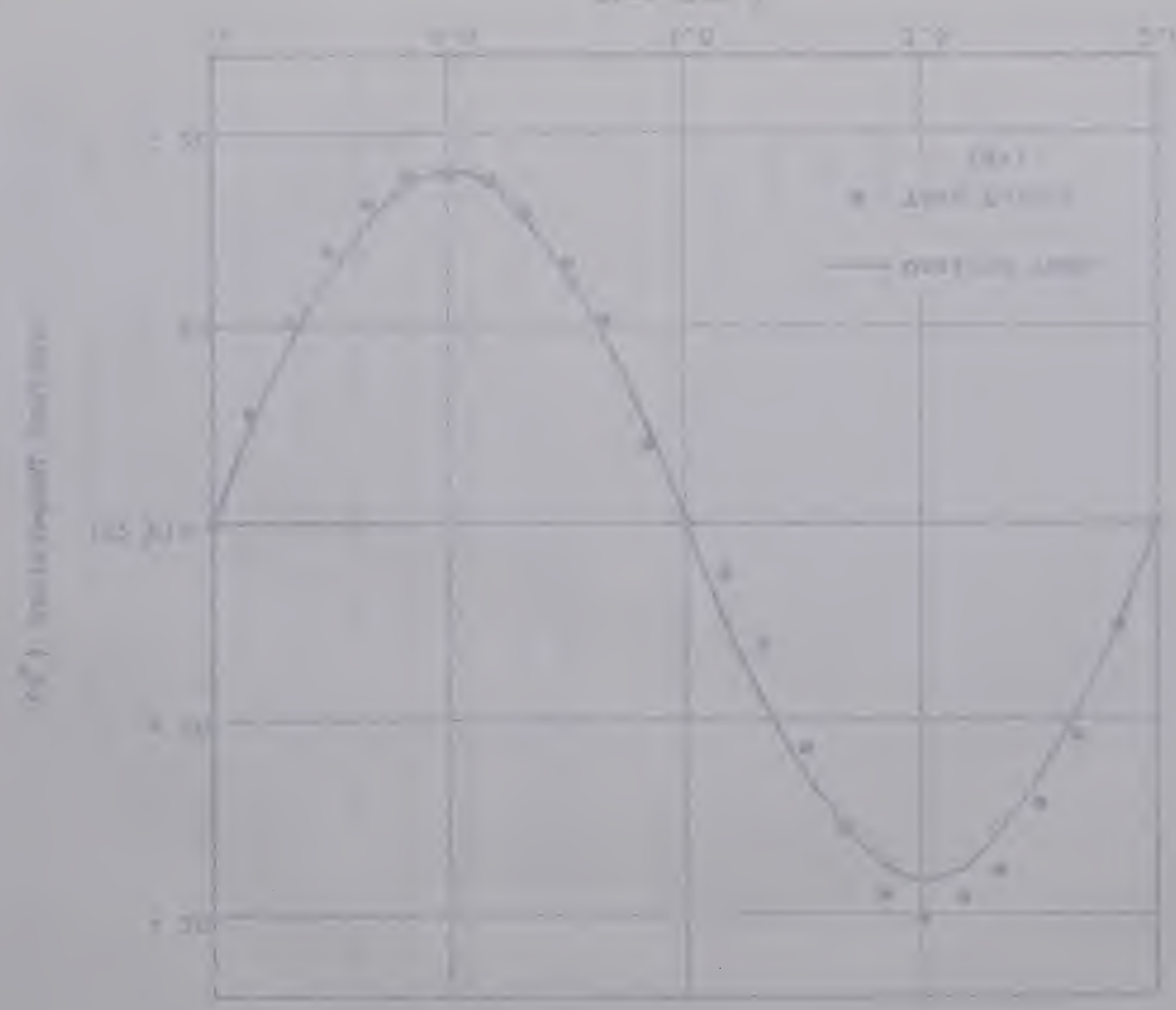

of the ice formation near each rod indicated that the thermal regime was influenced 1/8 inch radially outward from the rod surface. Hence the presence of the rods did not greatly affect the overall ice depth.

For a selected sinusoidual temperature amplitude of $\pm$ 18 °F, the reciprocal freezing temperature is $\Phi = 32.8$. Fig. 4.7 shows the experimental ice depth (test no. 2), clearly illustrating the regions of freezing and melting, over three complete cycles. Using these results and fig. 2.6, a comparison of "theory" versus experiment is given in table 4.1.

SINUSOIDUAL CYCLE DATA			VALUE OF β (ICE DEPTH)			
$\omega t=\alpha$ (Radians)	Sin α	θ_o (°F)	Theory	Cycle 1	Cycle 2	Cycle 3
0.2	.199	3.6	.045	.000	.055	.065
0.4	.389	7.0	.063	.027	.082	.094
0.6	.565	10.2	.077	.065	.096	.109
0.8	.717	12.9	.088	.090	.105	.118
1.0	.842	15.2	.096	.106	.111	.122
1.2	.932	16.8	.104	.114	.115	.124
1.4	.985	17.7	.110	.119	Ice layer added from Cycle 1	Ice layers added from Cycles 1 and 2.
1.6	.999	18.0	.116	.123		
1.8	.974	17.5	.119	.126		
2.0	.909	16.4	.123	.127		
2.4	.674	12.1	.128	.127		
3.0	.140	2.5	.132	.120		

TABLE 4.1 "THEORETICAL" VERSUS EXPERIMENTAL DEPTH OF FREEZING FOR PERIODIC CASE

The location of the melting interface for the second half-cycle is calculated by using the properties for water in the evaluation of Φ. Typical water properties are:

$$C_p = 1.005 \text{ BTU/lb}_m{}^\circ\text{F}$$
$$L = 144 \text{ BTU/lb}_m$$
$$\kappa = 0.0051 \text{ ft}^2/\text{hr}$$

Hence, for an amplitude, $\theta_m = \pm 18^\circ\text{F}$, the reciprocal melting temperature is $\Phi = 15.9$. Calculation of dimensionless ice depth is by

$$\beta \text{ ice} = \frac{b}{2\sqrt{\kappa_I t}} = \frac{2.23b}{\sqrt{t}}$$

whereas calculation of dimensionless melt depth is by

$$\beta \text{ water} = \frac{b}{2\sqrt{\kappa_w t}} = \frac{7.00b}{\sqrt{t}}$$

Table 4.2 furnishes the results for depth of melting.

SINUSOIDUAL CYCLE			(Based on Time Point) EXP. MELT DEPTH			THEORY	EXPERIMENT		
$\alpha=\omega t$	t	θ_o	b_1	b_2	b_3	β	β_1	β_2	β_3
rad	hr	°F	ft	ft	ft				
0.2	.064	3.6	-	-	-	.066	-	-	-
0.4	.127	7.0	.000	.002	.002	.091	.000	.039	.039
0.6	.191	10.2	.000	.008	.007	.110	.000	.128	.112
0.8	.255	12.9	.004	.011	.011	.125	.055	.152	.152
1.0	.318	15.2	.009	.014	.015	.138	.112	.174	.186
1.4	.445	17.7	.015	.019	.020	.158	.157	.199	.209
1.6	.510	18.0	.018	.022	.023	.165	.176	.215	.225
2.0	.636	16.4	.023	.025	.027	.176	.202	.219	.236
2.4	.765	12.1	.026	.028	.030	.181	.208	.224	.239
3.0	.955	2.5	.031	.032	.033	.184	.222	.229	.236

TABLE 4.2 "THEORETICAL" VERSUS EXPERIMENTAL DEPTH OF MELTING FOR PERIODIC CASE

Referring to fig. 4.7 and tables 4.1 and 4.2, the depth of freezing will be greater than the depth of melting; this arises from the difference in the averaged thermal properties of ice and water. Generally this difference exists for most materials. The difference in freezing and melting depths will occur using a sinusoidal surface temperature symmetrical* about a mean temperature at zero datum. Theoretically, equation (34) indicates that for assumed constant density across the interface, the ratio of freezing depth to melting depth is proportional to $K/\sqrt{\kappa}$ ignoring changes in the initial conditions. Using the thermal properties listed previously, the proportion

---

* Refer to page 24 footnote.

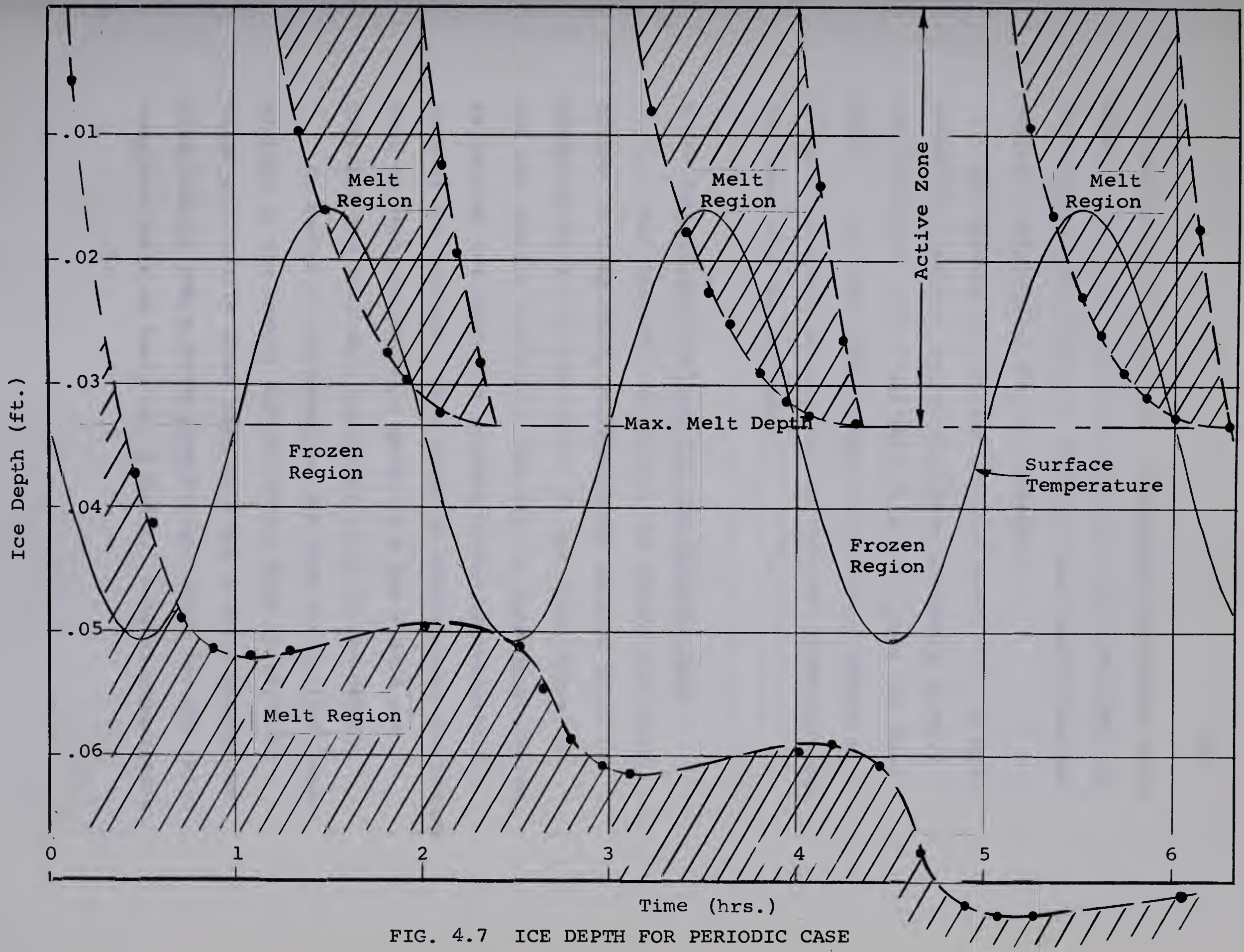

FIG. 4.7 ICE DEPTH FOR PERIODIC CASE

is calculated as 1.38:1.00. Considering the first cycle shown in fig. 4.7, the measured ratio is 1.59:1.00; the discrepancy may be due to imperfect test conditions and variable density across the interface.

The departure from the analytic model will be progressively greater as ice thickness increases because the "initial" conditions will change slightly for each cycle. For large depths, the ice bulk will behave as a "semi-infinite" domain with an "active" freezing/melting zone near the surface.

4.4-2 Temperature Profiles For the Periodic Case

It was observed that during the second and third cycles, no time delay (supercooling) existed prior to formation of a new ice layer. In the first cycle, no ice was present initially, whereas, in subsequent cycles, an initial ice layer was present within approximately 1 inch of the surface. This tends to substantiate the theory that no supercooling will occur if a few stable ice crystals are available somewhere close in the domain.

An analytic consideration was that the initial temperature in the domain (ice or water) must be at 32 °F. Table 4.3 clearly shows that this was a valid assumption. Experimental temperature profiles are shown for the third complete cycle of tests no. 1 and 2. Initial temperature

conditions are detailed at the zero and one hour time points. At zero time in each test, the position of the suspended ice layer remaining from the first two cycles may be noted in the temperature profile. The elevations of these layers were (at time zero):

Test no. 1 - ice layer .021 to .024 ft. below surface

Test no. 2 - ice layer .032 to .060 ft. below surface

The temperature oscillation at zero time of test no. 1 is not understood. With the experience from test no. 1, the second experiment was more carefully undertaken and hence, experimental justification of the initial condition is based primarily on test no. 2.

ωt	APPROX. TIME	SURFACE TEMP.	THERMOCOUPLE NO. 3	4	5	6	7	8	9	10	Remark
0	0	32.0	32.2	36.2	32.2	33.7	44.2	32.5	35.0	45.0	Test
π/2	½	26.0	30.2	33.5	32.2	34.5	41.0	32.5	36.2	43.2	No.1
π	1	32.0	32.0	32.0	32.0	32.5	37.0	32.0	33.5	39.0	
3π/2	1-½	41.7	32.2	32.2	32.0	32.5	37.2	33.0	33.0	39.5	
0	0	32.0	32.5	33.0	33.5	32.0	32.0	Inoperative	33.0	34.0	Test
π/2	½	14.0	17.0	20.0	21.0	25.5	29.5		32.5	33.0	No.2
π	1	32.0	31.5	32.0	31.5	31.5	31.5		32.0	32.5	
3π/2	1-½	52.0	39.0	33.0	33.0	32.0	32.0		32.0	33.0	
Thermocouple Depth			.0100	.0196	.0304	.0404	.0525	.0629	.0738	.0863	ft.

TABLE 4.3 TEMPERATURE PROFILES FOR PERIODIC CASE

4.5 RESULTS FOR TWO-DIMENSIONAL EXPERIMENTS

In the two-dimensional experiments, two adjacent surfaces were maintained at a uniform temperature; one surface was held at a temperature above freezing and the other below freezing. Only three experiments were undertaken. Firstly, for a particular temperature difference, the ice profile was allowed to form from an initially melted domain and then,it was compared with the profile obtained after thawback from an initially frozen domain primarily to establish that the profile had reached a stable curve. Secondly, the surface temperatures were lowered to develop another ice profile to illustrate any trend over the temperature range. Combined with this category was the comparison with a graphical solution, Brown [14], which is used to establish the 32°F isothermal with no regard to phase change or variations in properties. Finally, from temperature measurements at discrete points, the approximate location of isotherms were obtained.

4.5-1 Freezing Versus Thawback Ice Profile

The co-ordinates of the interface were measured easily by sighting along the plane of the interface. At every co-ordinate, the interface was exceptionally straight along the third axis. For reference, the

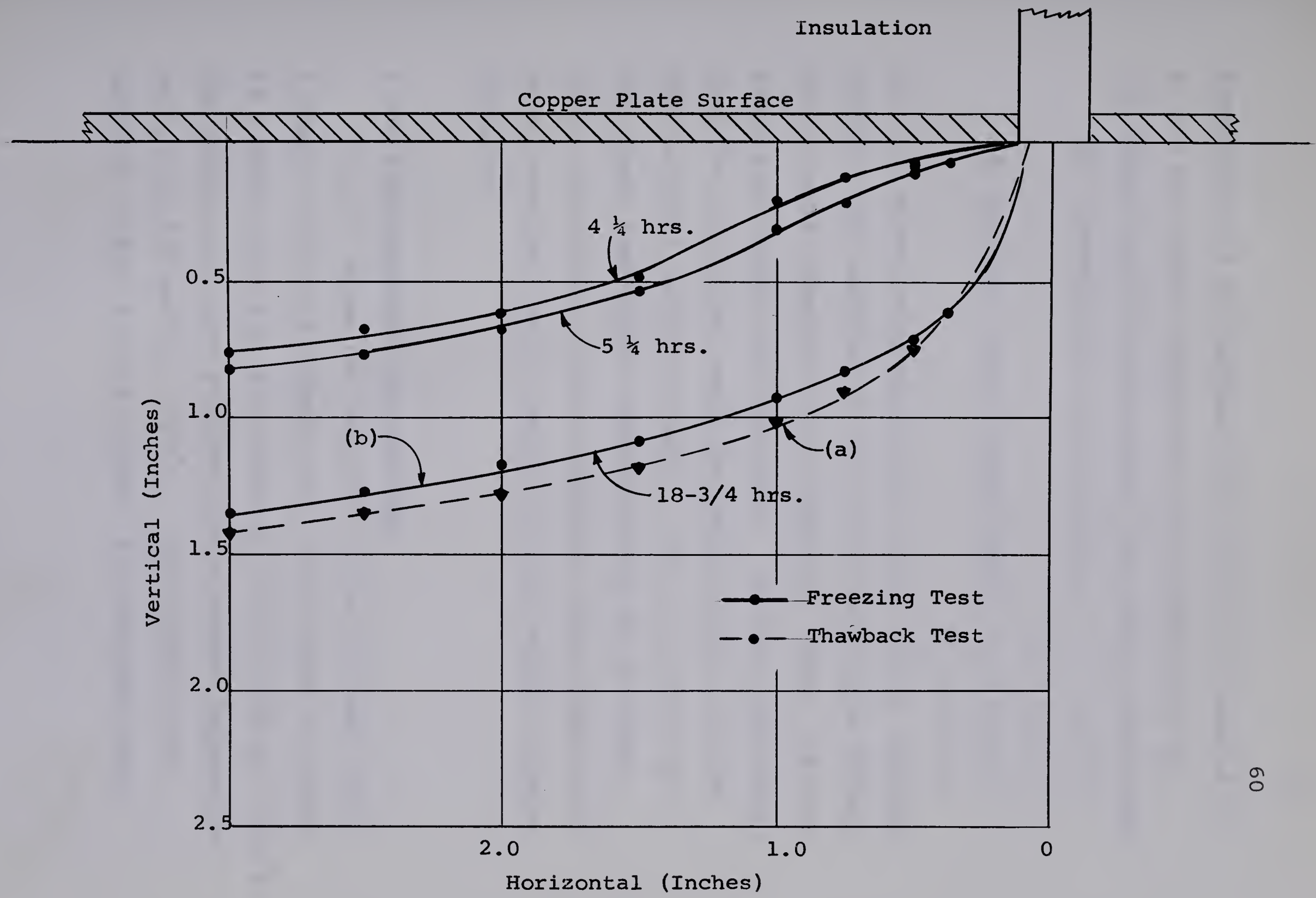

FIG. 4.8 FREEZING VERSUS THAWBACK ICE PROFILE

FOR TWO-DIMENSIONAL CASE

temperature of the surface below freezing is denoted by T_1 and the surface temperature above freezing by T_2. The temperatures in the thawback and freezing tests were:

(a) thawback from a frozen domain: $T_1 = 19.5\,^{\circ}F$, $T_2 = 59.5\,^{\circ}F$

(b) freezing, from a melted domain $T_1 = 20.5\,^{\circ}F$, $T_2 = 55.5\,^{\circ}F$.

Fig. 4.8 shows the resulting ice curves; nearly identical profiles were obtained for the given temperature difference, whether thawing back or freezing. Hence, the ice profile was stable for both tests. The plot also shows that the ice did not reach the centre of the 1/4 inch wide asbestos insulation board. This is a result of the linear temperature increase across the thickness of the insulation; a sharp temperature step change would be achieved only with a perfect thermal barrier of zero thickness.

4.5-2 Two-Dimensional Ice Profiles

Fig. 4.9 shows the variation in the ice depth with a change in surface temperatures. The thinner ice layer is a replot from fig. 4.8, where $T_1 = 19.5\,^{\circ}F$ and $T_2 = 59.5\,^{\circ}F$. The thicker ice layer resulted from a surface temperature of $T_1 = 10.5\,^{\circ}F$ and $T_2 = 36.5\,^{\circ}F$. Superimposed on the profiles in fig. 4.9 are typical $32\,^{\circ}F$ isotherms found

by the graphical method. These isotherms would result in a single phase (steady) system; they are based on a "geothermal" temperature gradient of 4 °F per inch which is close to the temperature gradient observed initially in the water. Even though the basis for the isothermal plot may not be truly representative of the particular system (for a single phase), it does reveal that the curvature of an isotherm is quite different for a two-phase system. This difference must stem from the variation in properties along the path of heat flux.

Shifting the temperatures, T_1 and T_2, to moderately lower values caused a substantial movement of the ice/water interface. A useful criterion for predicting the interface co-ordinates would be the ratio of temperature differences above and below the zero temperature datum, i.e. $(T_2 - A)/(A - T_1)$, where A is the melting temperature.

4.5-3 Two-Dimensional Isotherms

As previously stated, the temperatures at discrete points were used to find the approximate location of isothermal lines. The resulting isotherms are plotted in fig. 4.10. The "geothermal" gradient is noted to have a strong influence on the isotherms in the water region. In the ice region, the isotherms tend to follow the shape of the ice/water interface (+32 °F isotherm). The temperature gradient across the insulation panel is clearly revealed.

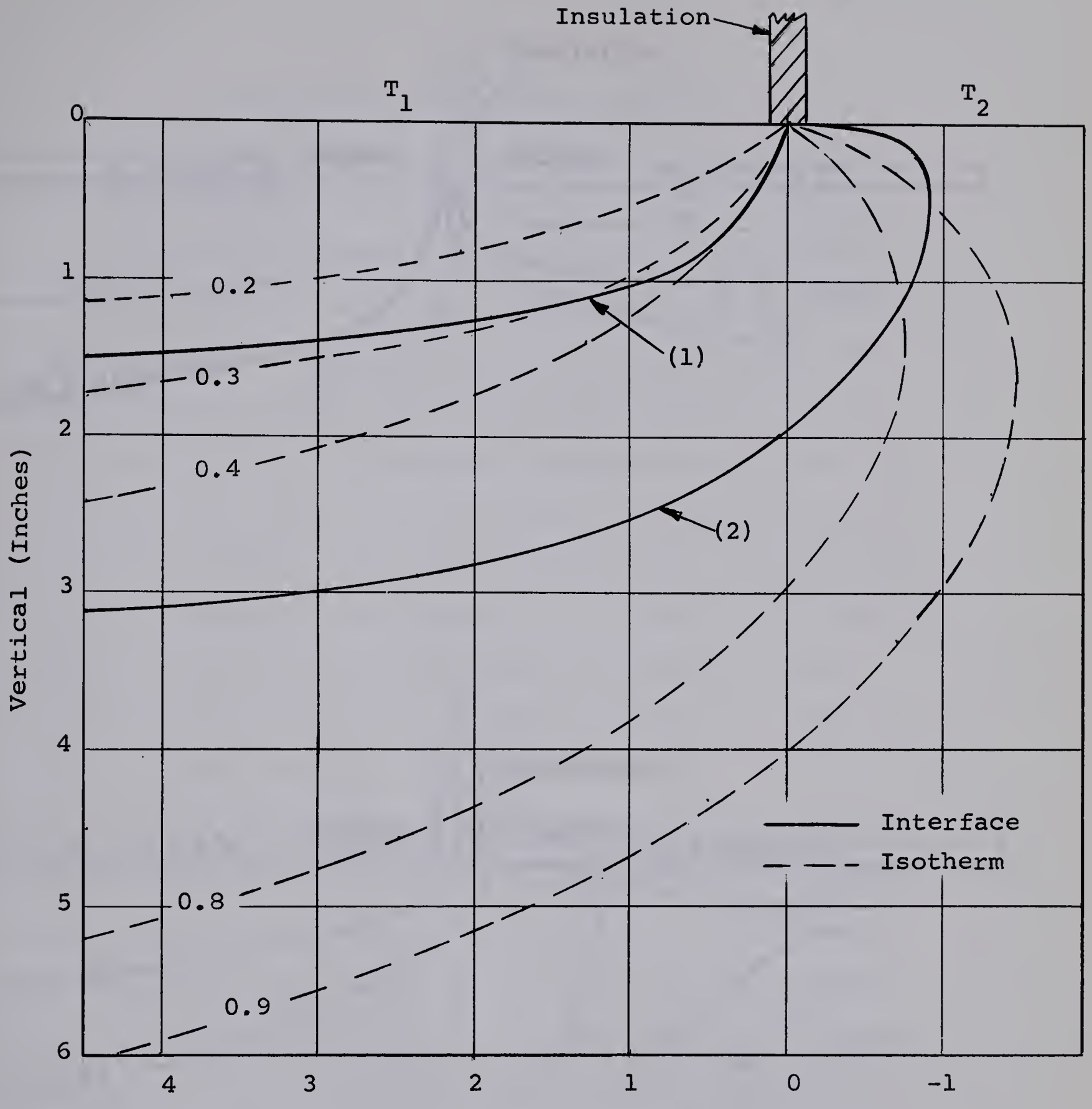

Interface (1): $T_1 = 19.5\,^{\circ}F$, $T_2 = 59.5\,^{\circ}F$ (Corresponding Isotherm 0.32)

Interface (2): $T_1 = 10.5\,^{\circ}F$, $T_2 = 36.5\,^{\circ}F$ (Corresponding Isotherm 0.83)

FIG. 4.9 GRAPHICAL DETERMINATION OF 32 °F ISOTHERM VERSUS ACTUAL INTERFACE LOCATION

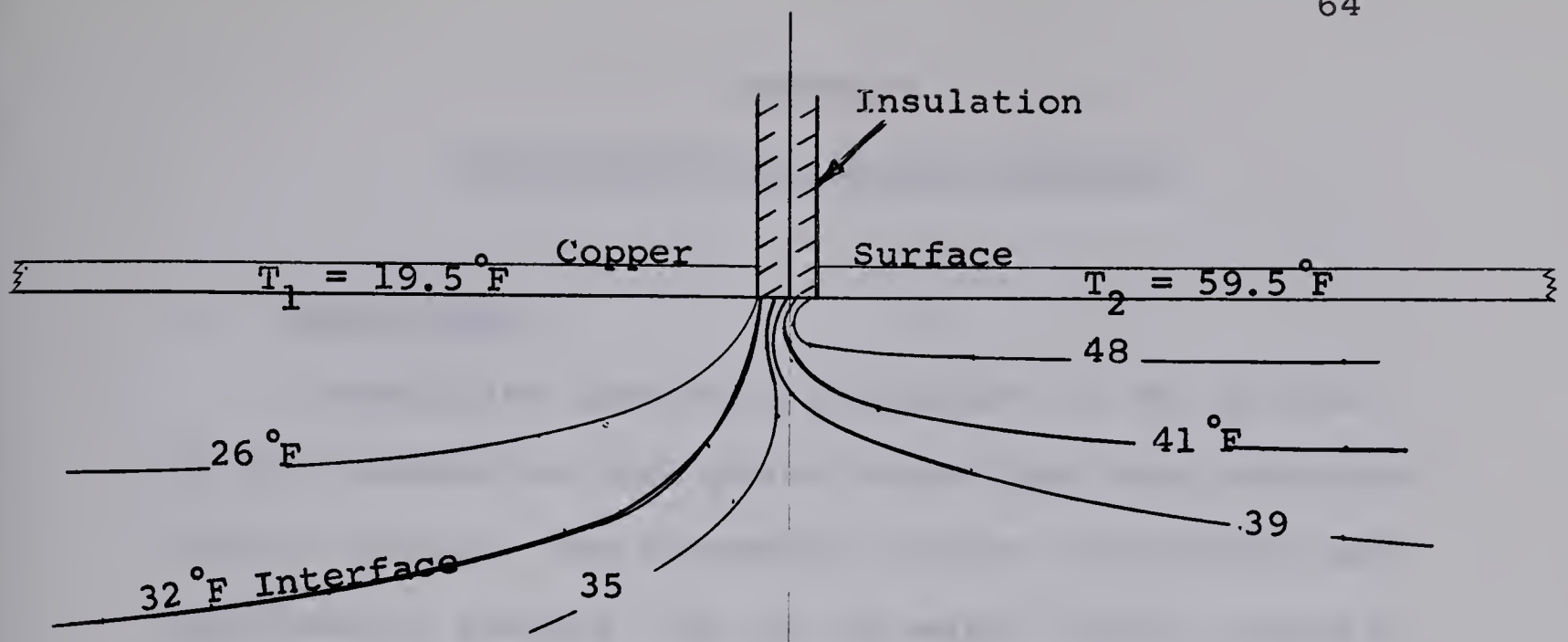

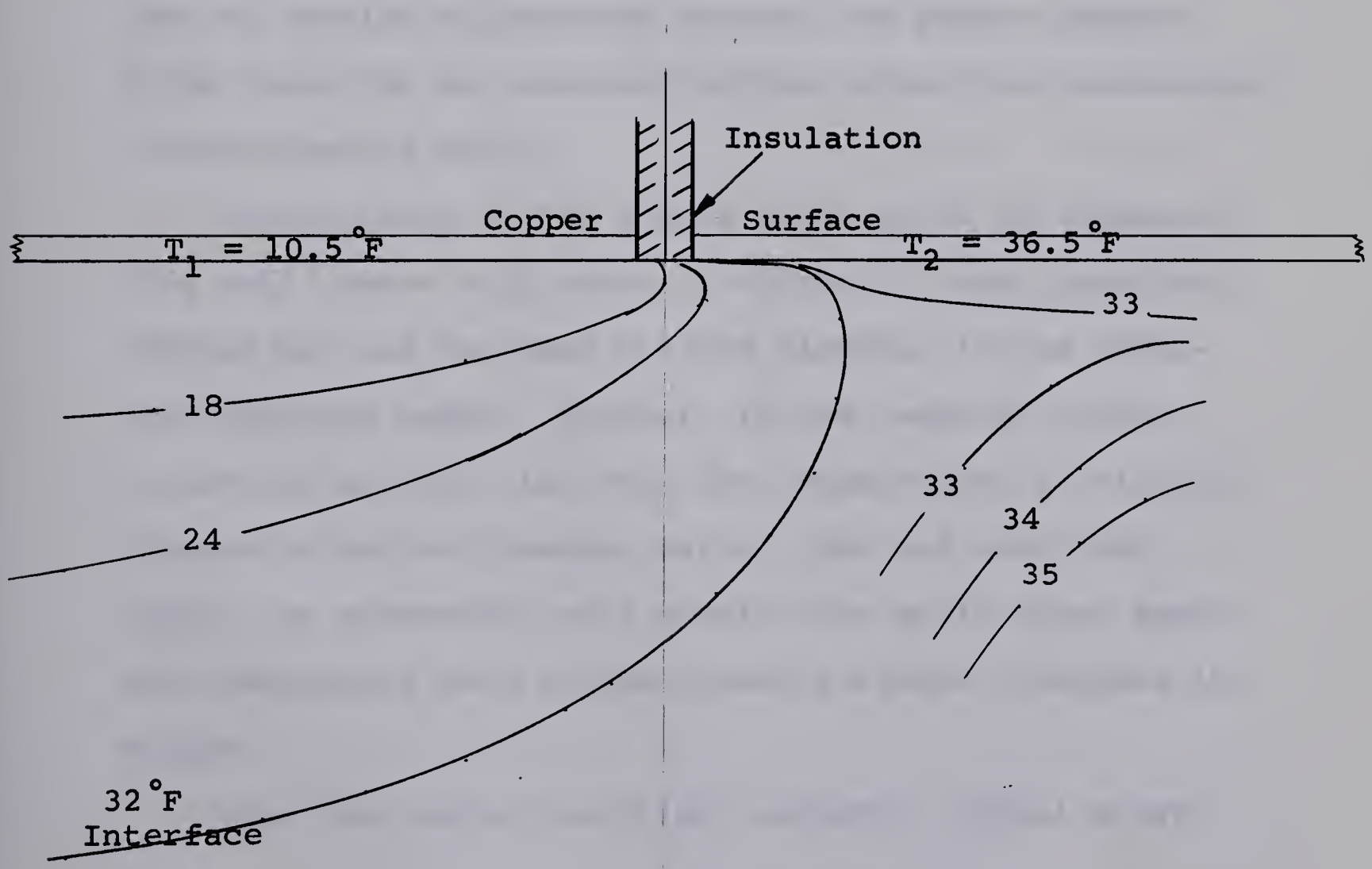

FIG. 4.10 STEADY TWO-DIMENSIONAL ISOTHERMS

CHAPTER V

CONCLUSIONS AND RECOMMENDATIONS

5.1 CONCLUSIONS

A simplified theoretical approach to the problem of heat conduction with phase change has been presented in this thesis. The agreement between theoretical and experimental results, for an ice-water system, using a power law variation of boundary temperature suggests that the idealized theory, as presented, is adequate for predicting ice depths and temperature profiles. In particular, the assumption of constant ice properties and neglect of density differences between the phases appears to be valid for an ice-water system within the limitations of experimental error.

Supercooling of the liquid phase prior to formation of a solid phase will occur in virtually every practical problem but has not been treated directly in the idealized analytic model. However, if the temporal origin is defined as that time when the temperature is initially reduced below the freezing datum, then the idealized theory, as presented, will predict the solid phase depth with reasonably good accuracy once a stable interface is formed.

With the latter condition realized, crystal growth

proceeds uniformly with the interface temperature remaining fixed at the stable equilibrium freezing point. If ice crystals are present in the water domain, as is evidently the case for the periodic surface temperature variation (after the first cycle), then no discernable supercooling will occur when the surface temperature is lowered below 32 °F.

An approximate power series solution has been presented for prediction of ice depth and domain temperature using the sinusoidual boundary temperature with the mean temperature at the freezing point. Experimental results indicate that the solution provides a fair prediction of the depth of freezing and melting for the first complete cycle. Theoretically and experimentally, it was shown that a "suspended" slab of the solid phase (ice) will be present after the first complete cycle and will be additive to the overall ice depth for the second complete cycle. If a positive temperature gradient exists in the liquid domain, then, the maximum ice depth will be reduced. The analytic solution, using the sinusoidual boundary temperature, may be expected to become progressively inaccurate after many cycles, as the ice thickness increases. This occurs because the initial domain temperature will not be zero at the beginning of each cycle.

The two-dimensional steady state experiments, using two adjoining flat surfaces at different (but uniform) temperatures above and below freezing respectively, reveal that the interface profile is quite different in curvature from that predicted graphically for the corresponding isotherm in a single phase system. This difference must result from the variation of thermal properties along the heat flow path in a two-phase system. The shape of the interface appears to be more sensitive to any change in the temperature of the surface above freezing. However, the co-ordinates of the two-dimensional steady profile possibly may be predicted solely by the ratio of surface temperatures above and below the freezing datum.

Based on the experimental evidence using an ice-water system, the test cell was larger than required for the particular investigation.

5.2 RECOMMENDATIONS

The simplified theory considers a domain which is initially at the fusion temperature only. The dimensionless formulation can be extended to include a uniform initial temperature higher than the fusion temperature. The case of a constant initial temperature gradient has not been investigated. The use of computers should

ultimately aid in the solution of the generalized time dependent boundary conditions for one-, two-, and three-dimensional work. In the meantime, there is a pressing need to extend the analytic solutions for practical boundary conditions as was done in the thesis for a sinusoidual variation.

Further experimental tests are required to confirm the simplified theory in such fields as casting of metals and frost penetration studies. For laboratory experiments with solidifying metals, the interface cannot be physically observed for depth measurements as was the case for an ice-water system. A closed, opaque container is required for the study of solidification of metals; as an example, mercury with its low melting point would require a relatively simple apparatus and consideration should be given to measuring the position of the interface on the basis of temperature only.

REFERENCES

1. CARSLAW, H.S. and JAEGER, J.C., "Conduction of Heat In Solids", Oxford Univ. Press, London, Second Ed., 1959, p. 282.

2. STEFAN, J., "Über die Theorie der Eisbildung, insbesondere über die Eisbildung im Polarmeare," Annalen der Physik und Chemie, Vol. 42, 1891, p. 269.

3. INGERSOLL, L.R., ZOBELL, O.S., and INGERSOLL, A.C., "Heat Conduction With Engineering and Geological Applications," McGraw-Hill Book Co., Inc., New York, N.Y., 1948.

4. LIGHTFOOT, N.M.H., "The Solidification of Molten Steels," London Math. Soc., Vol. 31, 1929, p. 97.

5. KREITH, F., and ROMIE, F.E., "A Study of the Thermal Diffusion Equation With Boundary Conditions Corresponding to Solidification or Melting of Materials Initially at the Fusion Temperature," Proceedings of the Physics Soc., Vol. 68, 1955, p. 277.

6. LANDAU, H.G., "Heat Conduction in a Melting Solid," Quart. of Appl. Math., Vol. 8, No. 1, 1950, p. 81.

7. MURRAY, W.D., and LANDIS, F., "Numerical and Machine Solutions of the Transient Heat-Conduction Problems Involving Melting or Freezing," Trans. ASME, May, 1959, p. 106.

8. GOODMAN, T.R., "The Heat-Balance Integral and Its Application to Problems Involving a Change of Phase," Trans. ASME, Feb., 1958, p. 335.

9. POOTS, G., "On The Application of Integral-Methods to the Solution of Problems Involving the Solidification of Liquids Initially at Fusion Temperature," Int. Jour. of Heat Mass Transfer, Vol. 5, June 1962, p. 525.

10. POOTS, G., "An Approximate Treatment of a Heat Conduction Problem Involving a Two-Dimensional Solidification Front," Internat. Journ. of Heat Mass Transfer, Vol. 5, May, 1962, p. 339.

11. PORTNOV, I.G., "Exact Solution of Freezing Problem With Arbitrary Temperature Variation on Fixed Boundary," Soviet Physics-Doklady, Vol. 7, No. 3, Sept., 1962, p. 186.

12. WESTPHAL, K.O., "On the Melting of Ice Sheets Under the Influence of a Bubbler System," Report B.I.O. 64-6 (Bedford Institute of Oceanography, Dartmouth, N.S., Canada,) Aug., 1964, "Unpublished Manuscript."

13. TURNBULL, D., "The Undercooling of Liquids," Scientific American, Vol. 212, No. 1, Jan. 1965, p. 38.

14. BROWN, W.G., "Graphical Determination of Temperature Under Heated or Cooled Areas on the Ground Surface," Tech. Paper No. 163, Div. of Building Research, Nat. Research Council, Ottawa, Oct., 1963.

BIBLIOGRAPHY

15. PERKERIS, C.L., and SLICHTER, L.B., "Problems of Ice Formation," Journal of Applied Physics, Vol. 10, 1939, p. 135.

16. LONDON, A.L., and SEBAN, R.A., "Rate of Ice Formation," Trans. ASME, Vol. 65, 1943, p. 771.

17. RUBENSTEIN, L.I., "On the Solution of Stefan's Problem," Bulletin del' Academie des Sciences de l'USSR, Vol. 11, 1947, p. 37 (Russian language.)

18. EYRES, N.R., HARTREE, D.R., INGHAM, J., JACKSON, R., SARGANT, R.J., and WAGSTAFF, J.B., "The Calculation of Variable Heat Flow in Solids," Philosophical Transactions of the Royal Society of London, Vol. 240, Series A, 1947, p. 1.

19. KERSTEN, M.S., "Thermal Properties of Soils," Bulletin No. 28, (Univ. of Minnesota,) 1949.

20. EVANS, G.W., "A Note on the Existence of a Solution to a Problem of Stefan," Quarterly of Applied Mathematics, Vol. 8, 1950.

21. RUDDLE, R.W., "The Solidification of Castings," The Institute of Metals, Vol. 77, 1950.

22. FORSTER, C.A., "Finite Difference Approach to Some Heat Conduction Problems Involving Change of State," English Electric Company Ltd., Report L.A.T. 059, 1954.

23. DOUGLAS, J., and GALLIE, T.M., "On the Numerical Integration of a Parabolic Differential Equation Subject to a Moving Boundary Condition," Duke Math. Journal, Vol. 22, 1955, p. 557.

24. OTIS, D.R., "Solving the Melting Problem Using the Electric Analog to Heat Conduction," Heat Transfer and Fluid Mechanics Institute, Stanford Univ., 1956, p. 29.

25. KOLODNER, I.I., "Free Boundary Problem for Heat Equation With Applications to Problems of Change of Phase," Comm. Pure and Applied Math., Vol. IX, 1956, p. 1.

26. LIEBMANN, G., "Solution of Transient Heat Transfer Problems by the Resistance-Network Analog Method," Trans. ASME, Vol. 78, 1956, p. 1267.

27. CITRON, S.J., "Heat Conduction in a Melting Slab," J. Aero Space Science 27, 1960, p. 219.

28. GOODMAN, T.R., "The Heat Balance Integral-Further Considerations and Refinements," ASME Paper No. 60-SA-9, 1960.

29. BOLEY, B.A., "A Method of Heat Conduction Analysis of Melting and Solidification Problems," Journ. of Math. Phys., Vol. 40, 1961, p. 300.

30. BIOT, M.A., and DAUGHADAY, H., "Variational Analysis of Ablation," Journ. of Aerospace Sci., Vol. 29, Feb., 1962, p. 227.

31. REDOZUBOV, D.V., "The Stefans Problem for a Linear Initial Temperature Distribution in a Semi-Infinite Medium," Bull. Acad. Sci., USSR Geophys. Ser. No. 4, April, 1962, p. 364.

32. OSTRACH, S., GOLDSTEIN, A.W., and HAMMAN, J., "An Analysis of Melting Boundary Layers on Decelerating Bodies," NASA TN D 1312, July, 1962.

33. BAXTER, D.C., "The Fusion Times of Slabs and Cylinders," Trans. ASME 84 C (Journ Heat Transfer) 4, Nov., 1962, p. 317.

34. GUTOWSKI, R., "The Problem of the Solidification Front In Liquids," Bull. Acad. Polonaise Sci., Warsaw, Vol. 10, No. 5, 1962, p. 183.

35. GEORGE, M.D., "On Mixed Problems For the Non-Linear Heat Equation," Journ. Math. Mech., 11, 6, Nov., 1962, p. 851.

36. THOMAS, L.J., and WESTWATER, J.W., "Microscopic Study of Solid-Liquid Interfaces During Melting and Freezing," University of Illinois, 1962.

37. MARTYNOV, G.A., "Principles of Geocryology," Part 1, Chap. VI, p. 153-192, Ac. of Sci., USSR, 1959, (Tech. Translation 1065, National Research Council of Canada, Ottawa, 1963.)

38. HAMILL, T.D., and BANKOFF, S.G., "Similarity Solutions of the Plane Melting Problem With Temperature-Dependent Thermal Properties," Industrial Eng. Chem.: Fundamentals 3,2 (Communication), May, 1964, p. 177.

39. HORVAY, G., "The Dip-Forming Process," Trans. ASME, Vol. 87, Series C, No. 1, 1965.

APPENDIX A

FORTRAN IV PROGRAMME FOR QUADRATURE SOLUTION

The Fortran IV programme, for ice formation, follows this introduction. Assuming numerical values for $\beta(\equiv L)$ and $n(\equiv D(J))$, the programme calculates corresponding values for the following, versus $\eta \equiv X(I)$:

$$fn(\eta) \equiv FU1\ (I)$$
$$Q'(\eta) \equiv VAR4\ (I)$$
$$Q(\eta) \equiv SAR3\ (I)$$
$$\tau \equiv A8$$
$$Ct^n \equiv A9$$

The particular constant, $\frac{\sqrt{\pi}\ L}{c_p} = 522.0 \equiv T$, has been used for ice. Changing this value only will allow calculations for steel, aluminum, and other materials.

```
      DIMENSION D(15),X(400),VAR(400),AR(400),SAR1(400),ERF(400)
      DIMENSION FU(400),VAR1(400),VAR2(400),SAR2(400),VAR8(400),AR1(400)
      DIMENSION VAR4(400),SAR3(400),AR2(400),VAR9(400),VAR5(400)
      DIMENSION VAR6(400),VAR7(400),DIF(400),FU1(400)
100   FORMAT(3X,F5.2,3X,F7.4,3X,F4.1,3X,F8.5,3X,F8.5,3X,F8.5,3X,F6.1)
101   FORMAT(5X,1HX,7X,2HFX,7X,1HN,7X,3HDQX,9X,2HQX,8X,4HTIME,8X,4HTEMP)
      WRITE(6,101)
      L=41
      C=0.01
      C1=0.2
      T=522.0
      J = 1
      D(J)=0.2
      K=1
      X(K)=0.0
1     X(K+1) = X(K) + C
      B=-(X(K)**2.0)
2     VAR(K)=EXP(B)
      IF (VAR(K) .LE. 0.00001) GO TO 3
      K=K+1
      GOTO1
3     K=1
      SAR1(K)= 0.0
4     AR(K) = (VAR(K) + VAR(K+1)) * C/2.0
      SAR1(K+1) = SAR1(K) + AR(K)
5     ERF(K) = 1.1283791 * SAR1(K)
      IF (ERF(K) .GE. 0.99998) GO TO 40
      K=K+1
      GOTO 4
40    K=1
41    VAR8(K) = ERF(K)/ERF(L)
      VAR9(K) = 1.0-VAR8(K)
      IF (K .EQ. L) GO TO 6
      K=K+1
      GO TO 41
6     I=1
      X(I) = 0.0
7     X(I+1) = X(I) + C
      B1 = -(X(I)**2.5)
      FU(I) = EXP(B1)
8     VAR1(I) = EXP(X(I)**2.0)
9     VAR2(I) = FU(I) * VAR1(I)
      IF (VAR2(I) .LE. 0.0001) GO TO 10
      I = I+1
      GO TO 7
10    I = 1
      SAR2(I) = 0.0
11    AR1(I) = (VAR2(I) + VAR2(I+1))*C/2.0
      SAR2(I+1) = SAR2(I) + AR1(I)
      IF (AR1(I) .LE. 0.00001) GO TO 12
      I = I+ 1
      GO TO 11
12    I = 1
13    VAR4(I) = SAR2(I) * VAR(I)
      IF (VAR(I) .LE. 0.00001) GO TO 15
      I = I + 1
      GO TO 13
15    I = 1
      SAR3(I) = 0.0
16    AR2(I) = (VAR4(I) + VAR4(I+1)) * C/2.0
```

```
      SAR3(I+1) = SAR3(I) + AR2(I)
      IF (AR2(I) .LE. 0.00001) GO TO 34
      I = I + 1
      GO TO 16
34    K = 1
35    VAR5(K) = VAR8(K) * SAR3(L)
      IF (K .EQ. L) GO TO 19
      K = K+1
      GO TO 35
19    I = 1
      K = 1
21    VAR6(I) = (SAR3(I) - VAR5(K)) * 4.0 * D(J)
22    FU1(I) = VAR9(K) + VAR6(I)
      IF (FU1(I) .LE. 0.0001) GO TO 23
      B3 = VAR2(I) / VAR1(I)
      DIF(I) = B3 - FU1(I)
      I = I + 1
      K = K + 1
      GO TO 21
23    DO 24 I=1,L
      IF (DIF(I) .GT. 0.0001) GO TO 26
24    CONTINUE
      A1=X(L)
      A2=A1**2.0
      A3=EXP(-A2)
      A4=A3/ERF(L)
      A5=(1.0+4.0*D(J)*SAR3(L))/(2.0*D(J)+1.0)
      A6=(0.8862269*4.0*D(J)*VAR4(L))/(2.0*D(J)+1.0)
      A7=A1/(A4*A5-A6)
      A8=A7**(1.0/D(J))
      A9=A7*T
      I = 1
      K=1
25    WRITE(6,100) X(I),FU1(I),D(J),VAR4(I),SAR3(I),A8,A9
      I=I+1
      K=K+1
      IF (I .EQ. (L+1)) GO TO 28
      GO TO 25
26    I = 1
27    VAR7(I) = FU1(I) * VAR1(I)
      VAR2(I) = VAR7(I)
      IF (VAR2(I) .LE. 0.0001) GO TO 10
      I = I + 1
      GO TO 27
28    J=J+1
      D(J)=D(J-1)+C1
      IF(D(J) .GE. 3.2) GO TO 36
      GO TO 19
36    L=L-5
      J = 1
      D(J)=0.2
      IF (L .EQ. 1) GO TO 30
31    K = 1
33    VAR8(K) = ERF(K)/ERF(L)
      VAR9(K) = 1.0 - VAR8(K)
      IF (K .EQ. L) GO TO 6
      K = K+1
      GO TO 33
30    STOP
      END
```

APPENDIX B

COMPARISON OF QUADRATURE AND EXPLICIT SOLUTION

The quadrature and explicit solutions can be compared by using both methods in the numerical evaluation of $fn'(\beta)$ in the basic equation (28). The quadrature solution for the temperature gradient at β is

$$fn'(\beta) = 4n\, Q'(\beta) - \frac{2}{\sqrt{\pi}} \frac{e^{-\beta^2}}{erf\beta} \left[1 + 4n\, Q(\beta) \right]$$

and the explicit solution is

$$fn'(\beta) = \frac{-2^{2n}\, \Gamma(n+1)\, e^{-\beta^2}}{Pn(\beta)\; i^{2n}\, erfc\, \beta} \quad .$$

The evaluation shall be undertaken for integer values $2n = 0, 1, 2$.

β	Quadrature $fn'(\beta)$			Explicit $fn'(\beta)$		
	2n = 0	1	2	2n = 0	1	2
.00	- ∞	- ∞	- ∞	- ∞	- ∞	- ∞
.05	(-)19.987	(-)19.979	(-)19.971	(-)19.987	(-)19.980	(-)19.969
.10	9.930	9.902	9.872	9.930	9.900	9.868
.15	6.568	6.522	6.477	6.568	6.519	6.472
.20	4.868	4.806	4.745	4.868	4.804	4.741
.25	3.836	3.759	3.684	3.836	3.758	3.681
.30	3.138	3.047	2.961	3.138	3.046	2.958

A comparison of β versus $fn'(\beta)$ shows that $fn'(\beta) \approx -1/\beta$ for all n. Substitution into equation (28) provides a second approximation for dimensionless ice depth, i.e.,

$$\beta = \left[\frac{\sqrt{\pi}}{2(2n+1)}\right]^{1/2} \tau^{n/2} \quad .$$

APPENDIX C

LAPLACE TRANSFORMATION METHOD

The Laplace transformation has been applied with considerable success to problems in heat conduction. The purpose of this section is to develop a general solution for the conduction equation with reference to the one-dimensional change of phase problem. A solution is sought for the differential equation (1) with boundary conditions

$$t = 0 \qquad 0 < x < \infty \qquad \theta = \theta_i$$

$$t > 0 \qquad x = 0 \qquad \theta = \theta_o(t)$$

$$t > 0 \qquad x = b \qquad \theta = 0$$

The Laplace transformation of equation (1) is

$$\frac{d^2\bar{\theta}}{dx^2} - \frac{S}{\kappa}\,\bar{\theta} + \frac{\theta_i}{\kappa} = 0$$

and the general solution for the transformed differential equation is

$$\bar{\theta} = A \sinh mx + B \cosh mx + \frac{\theta_i}{S} \tag{C1}$$

where S is the Laplace transform variable and $m = \sqrt{S/\kappa}$. The transformed boundary condition at $x = 0$ is $\bar{\theta} = \bar{\theta}_o(t)$. Substitution of transformed boundary conditions into equation (C1) yields

$$\bar{\theta} = \bar{\theta}_o(t) \left[\frac{\text{Sinh } m(b-x)}{\text{Sinh } mb}\right] - \frac{\theta_i}{s} \left[\frac{\text{Sinh } m(b-x) + \text{Sinh } mx}{\text{Sinh } mb}\right]$$

$$+ \frac{\theta_i}{s} \qquad \text{(C2)}$$

Considering the initial condition where $\theta_i = 0$, equation (C2) reduces to

$$\bar{\theta} = \bar{\theta}_o(t) \frac{\sinh m(b-x)}{\sinh mb} \qquad \text{(C3)}$$

The inversion of equation (C3) is presented here for the simple case of a linear variation in surface temperature.

Considering the temperature variation, $\theta_o = Ct$, the transformed temperature is

$$\bar{\theta} = \frac{C}{s^2}\left[e^{-mx} + e^{-m(x+2b)} + e^{-m(x+4b)} + \ldots\right] \qquad \text{(C4)}$$

Inverting (C4) term by term and substituting dimensionless variables where possible, gives

$$\theta = 4Ct\left[i^2\text{erfc}\eta + i^2\text{erfc}(\eta+2\beta) + i^2\text{erfc}(\eta+4\beta) + \ldots\right] \qquad \text{(C5)}$$

Using the energy balance equation (16) and differentiating (C5) term by term, the dimensionless depth, β, is found to be

$$\beta = \frac{2}{3}\tau\left[\sqrt{\pi}\left(\text{ierfc}\beta + \text{ierfc}3\beta + \text{ierfc}5\beta + \ldots\right)\right] \qquad \text{(C6)}$$

The "closed" form similarity solution for depth (20),

using n = 1, is

$$\beta = \frac{2}{3}\tau\left[\frac{e^{-\beta^2}}{2\beta^2 - 4i^2\mathrm{erfc}\beta + 1}\right] \qquad \text{(C7)}$$

A comparison of (C6) and (C7) is made in the table following; consideration need only be given to the numerical evaluation of the terms in the brackets. It can be seen that the series solution (C6) requires more terms for better accuracy.

β	[(C6) three terms]	[(C7) term]
0.00	∞	∞
0.05	2.2289	8.8485
0.10	1.7436	4.3728
0.15	1.3410	2.8677
0.20	1.0509	2.1010
0.25	0.8437	1.6312
0.30	0.6930	1.3108

APPENDIX D

A DISCUSSION ON DIMENSIONLESS DEPTH, β .

As stated in Chapter II and shown on fig. 2.5, the dimensionless ice depth tends to the limit of $\beta = 0.765$ and this corresponds roughly to a surface temperature, for all n, of $\theta_o(t) = -492\,^{\circ}F$. To illustrate, consider the ice property, $T^* = \sqrt{\pi}\, L/Cp$ or

$$T = \frac{\sqrt{\pi}\ (144)}{0.49} = 522 \text{ (units } ^{\circ}F)$$

For the maximum temperature step change, n = 0, and C = 492, it is found that

$$\beta_{max} = 0.945\ \frac{e^{-\beta^2}}{erf\beta} \approx 1.0\ \frac{e^{-\beta^2}}{erf\beta}$$

or $\beta_{max} \approx 0.765$. The case for $\theta_o(t) = Ct^n$ will be identical for calculating the limiting value, β_{max}.

As a comparison with other materials, the following table shows the approximate relation between the melting temperature and the constant, T:

---

* Used in Appendix A for the computer programme.

Material	Approx. Melting Temp. ($^{\circ}$R)	Value of T (handbook)
Ice	492	522
Aluminum	1680	1660
Copper	2440	1910
Iron	3262	3610
Lead	1080	695
Mercury	422	264
Silver	2220	1540

Since a considerable variation in thermal properties may be found in various handbooks on materials, there is some reason to believe that there should be actually a direct correspondence between melting temperature and the value of T.

From the tabulation, it may be seen that the constant, a, as defined in Chapter II, is of small order for materials other than ice. On this basis, a number of small order terms in equation (22) were neglected. From (22), the series solution,

$$\beta = \frac{2a\, t^{n}\, fn'(\beta)}{2n+1}\left[1 - \frac{\beta^{2} t^{-1/2}}{n} + \frac{\beta^{2}(\beta^{2}-1)\, t^{-1}}{n(n-1/2)} - \cdots\right],$$

was developed. The difficulty with this solution is that singularities occur at n = 0, 1/2, 1, ... However, for n = 0, the exact solution is known to be $\beta = 2at^{\circ}f_{o}'(\beta)$ and therefore only the first term in the series can be valid. The complete series solution appears to be valid

for non-integer values of n or for long time, t. Although not based on mathematical rigor but rather on the result from the case for n = 0, a solution seems possible if only those terms prior to the term containing the singularity are used. On this basis, for n = 1, the first three terms of equation may be used. Their relative values are shown in the table below, where an initial value for $\beta = \beta_o$ is assumed and time, t, calculated using the first term of the series. It is noted that the second and third terms are much smaller than one and therefore, the first term of the series is a good approximation for the evaluation of β.

		n = 1	a = -.00085 (ice)	
Assume β_o	$\frac{\beta_o}{fn'(\beta_o)}$	t	$\frac{\beta_o^2 t^{-1/2}}{n}$	$\frac{\beta^2{}_o(\beta_o^2 - 1)t^{-1}}{n(n - 1/2)}$
.00	.00000	0		
.05	.00250	4.41	+.00119	-.00001
.10	.01013	17.88	+.00236	-.00119
.15	.02316	40.87	+.00352	-.00190
.20	.04215	74.38	+.00463	-.00108
.25	.06786	119.75	+.00571	-.00144
.30	.10132	178.80	+.00673	-.00101

APPENDIX E

PROPERTIES OF TAP WATER.

Ordinary tap water, from the local region, was used in the experimental work. Typical values of chemical components are shown below for the month of January:

Component	River	Treated (Tap)
Hardness	241 (ppm)	88 (ppm)
Calcium	195	52
Magnesium	46	36
Alkalinity	197	29
Non-Carbonates	44	-
Ph	7.9	9.2
Total Solids	247	-
Suspended Solids	24	-